X-601-72-487
PREPRINT

A MODEL OF THE STARFISH FLUX IN THE INNER RADIATION ZONE

M. J. TEAGUE
E. G. STASSINOPOULOS

DECEMBER 1972

GODDARD SPACE FLIGHT CENTER
GREENBELT, MARYLAND

X-601-72-487
PREPRINT

A MODEL OF THE STARFISH FLUX IN THE INNER RADIATION ZONE

by

Michael J. Teague
The KMS Technology Center

and

E. G. Stassinopoulos
National Space Science Data Center

National Space Science Data Center
National Aeronautics and Space Administration
Goddard Space Flight Center
Greenbelt, Maryland 20771

December 1972

Page intentionally left blank

Page intentionally left blank

A MODEL OF THE STARFISH FLUX IN THE INNER RADIATION ZONE

by

Michael J. Teague
The KMS Technology Center

and

E. G. Stassinopoulos
National Space Science Data Center

ABSTRACT

A model of the Starfish electrons injected into the radiation belt in July 1962 has been determined for epoch September 1964. This model distinguishes between artificial and natural electrons and provides the artificial unidirectional electron flux as a function of equatorial pitch angle, energy, and L value. The model is based primarily upon data from the OGO 1, OGO 3, OGO 5, 1963-38C, and the OV3-3 satellites. Decay times for the Starfish electrons are given as a function of energy and L value. These decay times represent the best compromise between a number of independently determined values. The times at which the artificial Starfish flux component had become insignificant in comparison to the natural flux component are determined as functions of energy and L value. These times are determined by two separate methods, and averaged values are presented. It is shown that Starfish electrons, by the present time, have become insignificant for all energies and L values.

Page intentionally left blank

Page intentionally left blank

CONTENTS

ILLUSTRATIONS

ILLUSTRATIONS (continued)

ILLUSTRATIONS (continued)

Page intentionally left blank

Page intentionally left blank

NOTATION

Parameters

a	coefficients of polynomial fit to pitch angle distribution (Equation 3)
E	energy
E_T	energy threshold
f	solar cycle function (Equation 2)
j	unidirectional electron flux (Equation 1)
L	McIlwain parameter
N	AE-2 spectral function
p	flux ratio (Equation 4)
t	time
t_c	cutoff time (Equation 4)
T_s	time in months after Starfish injection
α-δ	coefficients of cutoff time function (Equation 7)
α_0	equatorial pitch angle
Θ	pitch angle parameter (Equation 3)
τ	Starfish decay time

Suffixes

d	data epoch
k	energy level
q	quiet day
st	Starfish
s	storm
o	time origin

I. INTRODUCTION

This document presents a model of the electrons artifically injected into the inner radiation belt by the Starfish nuclear explosion of July 1962. A complete description of residual Starfish electrons is given for epoch September 1964 with their corresponding decay times. These decay times are appropriate for the long-term loss process and do not apply to the relatively rapid degradation of the fission spectra immediately following the Starfish injection. The initial decay times are significantly shorter than the long-term values (Brown, 1965). Epochs are determined at which the decay of residual Starfish electrons became insignificant in proportion to temporal variations in the natural electron components of the inner radiation belt. These epochs are presented as functions of energy and L value and are referred to as cutoff times. Data from the following satellites were used in the development of the Starfish model: OGO 1, OGO 3, OGO 5, 1963-38C, OV3-3, Pegasus A and B, Explorer 26, Explorer 4, and Explorer 12.

At some general point in time after July 1962, the Starfish injection date, the total inner belt electron flux j can be expressed as

$$j = j_q + j_{st} + j_s \qquad (1)$$

where the suffixes q, st, and s denote the magnetically undisturbed (quiet day), the Starfish, and the storm time flux components, respectively. For much of the data analyzed in this document the storm component $j_s = 0$. However, for some energies and L values the presence of a significant storm component provided a useful method for determining the cutoff times. If the decay of the Starfish flux component is considered to be exponential with characteristic time τ, and the time

dependence of the quiet day component due to solar cycle variations is expressed as

$$j_q = j_{oq}\, f(t)$$

where the suffix o indicates some arbitrary time origin, then the change of the total population with time can be given as

$$\frac{dj}{dt} = j_{oq}\,\frac{df}{dt} + j_{oq}\,\frac{f}{\tau} - \frac{j}{\tau} \qquad (2)$$

Note that it is implicit in Equation 2 that τ is time independent. A complete description of the quiet day flux solar cycle variations has been given by Teague and Vette (1972). For most of the time period considered in the present study, df/dt is positive. Thus, the first two terms of Equation 2 represent source terms, and the third term represents a loss term. The variable τ will be referred to as a decay time and relates to the net depletion rate of electrons as opposed to their actual lifetime. This distinction arises as a result of cross L and pitch angle diffusion. Since the diffusion equation is linear, separation of the quiet day and Starfish components can be performed, and the two components can be studied separately.

In Section II of this document, a brief description of the iterative procedure for the separation of the flux components j_q and j_{st} is given. A more comprehensive description has been given previously by Teague and Vette (1972). Polynomial fits are obtained for the pitch angle dependence of the Starfish component, and flux levels are presented as functions of L value for discrete energy ranges in the energy interval $133 \leq E \leq 4740$ keV. In Section III the decay time model is presented. Values of τ are determined from the OGO 1 and OGO 3 University of Minnesota electron spectrometer data (Pfitzer, 1968) and from the 500-keV Explorer 26 data (Teague and Vette, 1972). These decay times and those previously given by Rosen and Sanders (1971), based

upon measurements from Pegasus A and B, and by Farley (1969), based upon measurements from Explorer 15 and OV1-2, are compared with the Stassinopoulos and Verzariu decay time model (1971). An average decay time model is determined. In Section IV the cutoff times are presented. These quantities are possibly the most important ones presented in this document from a practical viewpoint, and two distinct methods are adopted for their determination. The first method relies upon the separation of the various flux components given in Equation 1 and defines a cutoff time as the time at which the artificial and natural components are equal. The second method is more qualitative and uses data from the 1963-38C satellite exclusively. This method uses the appearance of a significant storm component or the decay of the total flux to the proton background for initial estimates of the cutoff times. Refined values are obtained iteratively by precluding inversions in the energy spectrum at any given time. In the regions where extrapolations are performed by both methods, estimates are made for the cutoff times by using the upper limits of the pre-Starfish electron fluxes given by the Explorer 4 and 12 satellites. Qualitative confirmation of the final cutoff times is obtained by comparing the Starfish model with data from the OGO 5 and OV3-3 satellites.

Page intentionally left blank

Page intentionally left blank

II. THE STARFISH FLUX MODEL

The primary data used for determining the Starfish model were those measured by the OGO 1 and 3 electron spectrometers (Pfitzer, 1968). Data from the OV3-3 electron spectrometer (Vampola, 1969), the OGO 5 electron spectrometer (West et al., 1969), and the 1963-38C integral detectors (Beall, 1969) were used for confirming this model. The energy ranges covered by these detectors and the types of measurements are given in Table 1. For the OGO 1 and 3 and the 1963-38C satellites, the energy ranges given in Table 1 differ from those originally used by the principal investigators. A full description of the reevaluation of the calibration of these detectors is given by Teague and Vette (1972) and by Teague (1970). For the OGO 5 satellite, the original energy ranges and geometric factors given by West et al. (1969) are used. For the OV3-3 satellite, the energy ranges are those given by Vampola (1969). However, the geometric factors for OV3-3 have been increased by a factor of four (Vampola, private communication).

The quiet day and Starfish components were separated in the following iterative manner: (1) by using OGO 1 data as near to the Starfish epoch as possible (September 1964), an initial value of τ was determined with the assumption that $j >> j_{oq}$ in Equation 2; (2) the flux was decayed using this value of τ until the observed total flux was larger then the decayed flux by at least a factor of three (the difference of these fluxes approximates the quiet day flux component at the epoch of the comparison); and (3) then, using this quiet day flux value, an estimate of the quiet day flux at the epoch of the initial τ determination was made, and an improved τ value was determined from Equation 2. The iteration process is lengthy, and many iterations are not warranted because significant errors may be

introduced by extrapolating for the quiet day flux. In practice, however, this extrapolation was assisted by observations at L values and energies for which $j_q >> j_{st}$, and observations of f(t) can therefore be made.

The OGO 1 and 3 data sets provided unidirectional flux as a function of energy, L value, and time; therefore, a second iterative procedure was adopted to remove the pitch angle dependence. In most cases decay times are presented using the approach described in this section for equatorial fluxes on the assumption that τ is B independent. This assumption is borne out by the Stassinopoulos and Verzariu (1971) decay model for $L \geq 1.4$. As each step of the previous iteration cycle, the following procedure was adopted. For every value of energy and L, (1) an approximate determination of the pitch angle dependence was made using the month of data affording the best pitch angle coverage; (2) data from all epochs were normalized to the equator using this pitch angle dependence, and initial values of τ were determined; (3) these values of τ were used to normalize all data to a common epoch assuming that τ was B independent, and an improved pitch angle distribution was obtained; and (4) this average pitch angle distribution was then used to obtain an improved value of τ. As with the previous iteration technique, many iterations are not warranted because of the accuracy of the technique and the standard deviation of the data points.

A typical example of the result of the iteration procedures, demonstrating the separation of the quiet day and the Starfish components of the flux, is shown in Figure 1 for L = 1.5 and 1.9 and for $292 \leq E \leq 690$ keV corresponding to one energy range of the OGO 1 and 3 satellites. Curves for the two flux components and the total flux are shown with the Starfish flux data from the OGO 1 satellite covering the period September 1964 to April 1965. Representative averaged quiet day flux data from the OGO 3 satellite covering the periods June 1966 and

December 1967 are also shown in Figure 1. At the lower L value, the dominant component at the earlier time period is clearly j_{st}. At the higher L value the quiet day component is starting to become significant in late 1964, and the decay time determined assuming $j_{st} >> j_q$ is significantly different from the more correct value obtained from Equation 2 as discussed in Section III.

Simple polynomial fits were made to the equatorial pitch angle distribution of the Starfish flux given by the OGO 1 and 3 data that were normalized to the epoch of September 1964 using the expressions

$$\log_{10} (j_{st}) = a_0 + a_1(\Theta-\alpha_0) + a_2(\Theta-\alpha_0)^2 + a_3(\Theta-\alpha_0)^3$$

$$\text{for } \alpha_0 \leq \Theta$$

and (3)

$$\log_{10} (j_{st}) = a_0 \text{ for } \alpha_0 > \Theta$$

where α_0 is the equatorial pitch angle and Θ is an L-dependent parameter for the pitch angle function. The L-dependent constants a_0, a_1, a_2, a_3 and Θ are shown in Table 2 for the four higher energy ranges covered by the OGO 1 and 3 spectrometers. No comparisons are shown here between the OGO 1 and 3 data and Equation 3 because these comparisons have been reported previously by Teague and Vette (1972). No coefficients are presented for the lowest energy range $36 \leq E \leq 133$ keV because it was clear from the data that no Starfish residual remained at these energies in late 1964, with the possible exception of $L \leq 1.3$ earth radii. The data yielded little information concerning the component j_q for the two highest energy channels of the OGO 1 and 3 spectrometer, and both the polynomial fits and the decay times were determined assuming that $j_{st} >> j_q$. However, crude estimates of j_q for $E > 690$ keV were

obtained from the OV3-3 data, and the assumption of $j_{st} >> j_q$ proved to be adequate for L < 1.7 earth radii. For higher L values the iteration procedure described in Section I was adopted using the estimated j_q values from OV3-3.

At low (L < 1.5) and high (L > 2.0) L values the pitch angle dependence of j_{st} is appreciably flatter than j_q. At intermediate L values the pitch angle dependence is very similar (Teague and Vette, 1972).

This analysis has been performed assuming that the storm component $j_s << j$. For L ≥ 2.0 earth radii and 292 ≤ E ≤ 690 keV, however, the effects of the magnetic storms occurring on February 7, 1965, and April 18, 1965, are evident (Teague and Vette, 1972), and it is possible that the Starfish flux determined for September 1964 contains a significant storm component. The effects of magnetic storms are evident in the 1963-38C low-energy data for 1964 for L > 2.0; however, for all other L values and energies shown in Table 2, no significant storm effects were observed in the OGO 1 data.

III. AVERAGE DECAY TIMES

Table 1 shows the energy ranges in which the OGO 1 and 3 data provided a measure of the residual Starfish flux component, and the decay times for these energy ranges are presented in Table 3. Note that no values are given for L = 1.3 because the time coverage of the OGO 1 data was poor. The decay times for L > 2.0 earth radii and $292 \leq E \leq 690$ keV must be regarded as approximate because of the magnetic storm effects described in Section II. The quoted values are based upon the average of the decay times observed before and after the February storm. The variation of τ on either side of the storm was less then 4%. The error of the decay time is related to the data time sample, the standard deviation of the data, and the significance of the quiet day component over the time sample. Estimates of the errors are presented in Table 3. The error increases towards the lower L values primarily because the time sample decreases.

The OGO based decay times can be compared with the decay time model of Stassinopoulos and Verzariu (1971). As noted previously, their decay time model is based upon data from the 1963-38C satellite. Threshold energies for the three channels are taken as E_T = 255 keV, 1.34, and 2.4 MeV (Teague and Vette, 1972). Nominal thresholds of 280 keV, 1.2, and 2.4 MeV were used in the derivation of the Stassinopoulos and Verzariu model; however, it is not considered that these threshold differences introduce significant errors into the present analysis. The Stassinopoulos and Verzariu model is analytic, provides τ (B, L, E_T), and is valid in the energy range $200 \leq E \leq 3000$ keV approximately. The model provides B dependence of τ for L < 1.4 earth radii. For comparison with their model, the OGO Starfish flux components were summed to provide integral fluxes for E_T = 133, 292, 690, and 1970 keV. Integral flux decay times were determined and are compared with the values of

the Stassinopoulos and Verzariu model in Table 4. Estimates of the errors for the present values are included in Table 4. The error of the Stassinopoulos and Verzariu model is given as ±15 days. Two decay times are given from this model at L = 1.3 earth radii, the higher value corresponding to the equator and the lower value to B = .22 gauss (atmospheric cutoff = 0.232 gauss approximately). For the two highest energies there is substantial agreement between the two models for τ. At 292 keV however, there is considerable disagreement for L < 1.8 earth radii. Two reasons exist for differences between the two τ values: (1) the effect of the background flux, which was not included in the Stassinopoulos and Verzariu model, and (2) the variation of the decay time with time. In Figures 2 through 8 the flux decay times based on OGO data are shown with values based upon the 500-keV Explorer 26 data (Teague and Vette, 1972). Those decay times given by Rosen and Sanders (1971) are based upon measurements by the Pegasus A and B satellites for 500 keV and 300 keV respectively, and those decay times given by Farley (1969) for 500 keV are based upon measurements from the Explorer 15 and OV1-2 satellites. In addition, the present model and the Stassinopoulos and Verzariu model are shown. Only the OGO values in these figures have been determined after removal of the quiet day background flux.

Approximate error bars are given for each measurement except for Farley's measurements for low L values. For L < 1.35 and L > 1.5, Farley's measurements indicate B dependence of τ. For L > 1.5 the variation of τ with B indicated by Farley is small and may result from measurement error, and these variations are shown as error bars on the data. No other error information is available for Farley's data. For the lower L range, B dependence is also indicated by the Stassinopoulos and Verzariu model, shown on Figures 2 through 8 as broken lines.

No clear picture emerges from the comparison of the various data on Figures 2 through 8, and it is evident a priori that any compromise model will show significant disagreement with one or more sets of data. A possible explanation for the large data spread may be the different epochs of the measurements and the variation of the decay time with time. The OGO 1, Pegasus A and B, and Explorer 26 data span the period from late 1964 to late 1965, Farley's data span the period from early 1963 to late 1965, and the Stassinopoulos and Verzariu model spans from late 1963 to mid 1965. However, since Figures 2 through 8 indicate no consistent trend for the variation of τ with time, this explanation is unlikely. As noted, it is clear from Table 4 that the principal differences between the Stassinopoulos and Verzariu model and the OGO 1 and 3 based decay times occur for $L \leq 1.8$ at 292 keV. To a lesser extent, differences are also observed at 690 keV for $L \leq 1.6$. As reported by Teague and Vette (1972), for these energies and L values, at the epoch of the decay time determination from the OGO data, approximately 90% of the total flux is residual Starfish flux. Therefore, the removal of the quiet day background from the total flux before calculation of the decay time from the OGO data does not explain the differences observed in Table 4. Removal of the quiet day background will affect the final integral decay times for 133-keV electrons for $L > 1.6$ and for the higher L values at higher energies. The differences observed between the various decay times on Figures 2 through 8 must result largely from statistical variations in the data, and the error bars quoted for both the OGO based decay times and the Stassinopoulos and Verzariu model must be regarded as somewhat optimistic in these regions.

With the exception of $L = 2.2$, the available calculated decay times generally lie considerably below the Stassinopoulos and Verzariu model for $E_T \lesssim 500$ keV, and an average model should exhibit that characteristic. Further, as noted previously, at 1970 keV the OGO data and

the Stassinopoulos and Verzariu model agree substantially, and an average model should be asymptotic to this model at high energies. The resulting decay time model is shown in Figures 2 through 8 as full lines. This model covers the L range $1.2 \leq L \leq 2.2$ and the energy range $0.1 \leq E_T \leq 3.0$ MeV, and indicates an approximate B dependence for $L \leq 1.3$. The major differences between the two decay time models occur at low energies, and for $L > 1.4$, agreement with the various data is fair. Reasonable figures for the present model error may be ±40 days for $E_T < 600$ keV approximately and ±25 days for high energies. For $L \leq 1.4$ earth radii (Figures 2 through 4), considerable variation in τ is observed among the various data sets, and the model error may be as high as ±60 days for $E_T < 500$ keV. A threshold-energy vs L-value decay time map summarizing the model is presented in Figure 9. For $L < 1.4$ earth radii, both equatorial values and estimates of τ at higher B values may be obtained from Figures 2 and 3. It can be seen in Figure 9 that the maximum decay time is about 380 days occurring at $L = 1.45$ and $E_T = 1$ MeV approximately.

It is possible to obtain confirmation of the Starfish flux model based primarily on OGO 1 and 3 data (Table 2) by use of the 1963-38C data. Figures 10 and 11 compare the Starfish model integral spectra with the 1963-38C data for epochs January 1965 and June 1966. Approximate error bars are indicated for the data and the model. The model error in June 1966 is significantly greater than that at the earlier epoch as a result of extrapolation using the decay time model described in the previous paragraph. The 1963-38C and OGO data have been corrected for quiet day background. In general, it can be seen that the agreement at both epochs is good. Note that minor differences may be observed between Figures 10 and 11 and similar figures previously presented by Teague and Vette (1972). These differences arise because of the use of a slightly different decay time model in the previous analysis performed by Teague and Vette (1972).

IV. CUTOFF TIMES

One of the purposes of this document is to determine if the residual Starfish fluxes discussed in the previous section have become insignificant in relation to the natural content of the inner radiation belt for the present epoch. It is already evident from Table 2 that no Starfish residual was observed in September 1964 for electrons with energies 36 to 133 keV, and that residual electrons with E > 2 MeV have become insignificant by the same epoch at high L values.

Two different approaches were adopted for determining the cutoff times. Method 1 relies upon the separation of the natural and the Starfish flux components that has been discussed in the preceding sections. Method 2 is a qualitative approach using data from the 1963-38C satellite. The two methods provide useful comparisons in some regions. In other regions the cutoff times can be determined only by one method or the other. Each method is discussed separately, and a final averaged cutoff time model is presented.

A. Method 1

As an index of the significance of the Starfish flux component, a time dependent variable p is introduced as

p(t) = Starfish flux component at time t/total flux at time t.

For regions for which the storm component remains insignificant, a cutoff time t_c may be given as

$$t_c = \tau \log_e \left\{ \frac{[1-p(t_c)]\ j_{st}(t=0)}{p(t_c)\ j_q(t_c)} \right\} \qquad (4)$$

Since both j_q and j_{st} are time dependent, Equation 4 must be solved by iteration. The accuracy of the Starfish model and the quiet day component are such that solution of Equation 4 is not warranted for $p < 0.5 (j_{st} = j_q)$. The accuracy of t_c depends upon the value of t_c and the error associated with (1) the decay time model, (2) the Starfish flux model for epoch September 1964, (3) the solar cycle dependence of the quiet day model (Teague and Vette, 1972) and the quiet day model itself, and (4) magnetic storm effects. In practice, because the errors in t_c resulting from errors in τ increase with the extrapolation time, this source of error is the most important for most L values and energies. However, at high L values or high energies, error sources (3) and (4) become important.

Sets of cutoff times have been presented previously by Teague and Vette (1972) for both differential and integral fluxes using the OGO based decay times. In the present document the decay time model discussed in the previous section is used, and the times t_c for which the Starfish flux component is equal to the natural quiet day component ($p = 0.5$) are shown in Table 5 for the energy thresholds corresponding to the OGO 1 and 3 detectors. Since large differences are evident in the decay time data discussed in the previous section, and since errors in this parameter are most important in the accuracy of the cutoff times, this parameter is also computed using the OGO based decay times and the Stassinopoulos and Verzariu model. In Table 5, t_c is shown as month and year and also as T_S, month from Starfish injection (July 1962). Errors are presented for the values determined with the present decay time model. As noted previously, no residual Starfish flux in the energy range $36 \leq E \leq 133$ keV was observed in late 1964, and the values of t_c given in Table 5 for $E_T = 36$ keV represent the decay process for Starfish particles with energies $E > 133$ keV. Note that no cutoff times are given for $L = 1.2$ since the Starfish flux model (Table 2) is valid for the L range $1.3 \leq L \leq 2.2$ only. As would be expected from the

Starfish model, in most cases the cutoff times decrease with increasing L at any energy. Further, the peak cutoff time in Table 5 at any L value occurs at E_T = 690 keV approximately. The cutoff times given for L = 1.3 are determined at the equator. At higher B values the decay time is reduced (Figure 3), tending to give smaller values of t_c. However, the Starfish component pitch angle dependence is flatter than the quiet day component at L = 1.3 (Teague and Vette, 1972), tending to cause the reverse trend. It is considered that any variation of t_c with B at L = 1.3 is smaller than the errors quoted in Table 5.

It is emphasized that the above cutoff times have been determined using the quiet day background with the assumption that $j_s \ll j$. Storm effects influence these times for two reasons. First, magnetic storms are observable in the data at epochs much earlier than t_c with the result that the Starfish component flux model presented in Table 2 may be an overestimate of this component in September 1964. This effect is most likely to occur at the higher L values and intermediate energies. Second, as magnetic storm effects provide a significant contribution to the total natural flux in the inner belt, it is clear that the quiet day component is an underestimate of the effective background flux. Both those effects (i.e., an overestimate of the Starfish component in late 1964 and an underestimate of the effective background flux) will result in values of t_c that are too large, particularly at high L values and intermediate energies. The errors quoted in Table 5 do not attempt to account for this error source, and the values of t_c presented in this table must be regarded as maximum values for p = 0.5.

B. Method 2

For Method 2, the determination of the cutoff times was based entirely upon data from the 1963-38C satellite (Beall, 1969). For this portion of the analysis, the assumed electron energy thresholds were

taken as 0.28, 1.2, and 2.4 MeV. As already noted, the small differences in energy threshold assumed do not contribute a significant error to the analysis.

As indicated in Table 1, the 1963-38C detectors measured protons above 150 MeV approximately, in addition to electrons, and observations of the data from the two higher energy channels (1.2 and 2.4 MeV) indicated that the total flux decayed to the proton background. Therefore, the possibility existed that the electron decay process was masked by the proton background. For the lower energy channel (.28 MeV) a significant storm contribution j_s was observed at the latter stages of the decay process. Due to the relative sensitivities to electrons and protons, no storm effects were observed at the higher energies.

Initial estimates of the cutoff times were obtained as those times for which the total flux decayed to the proton background for the two higher energy channels and the times at which observable storm effects were evident for the low energy channel. It was noted in Section II for $L < 1.8$ at energies comparable to those measured by the 1963-38C low energy channel, that the storm flux component $j_s \ll j_{st} + j_q$. In the present context therefore, an "observable" storm effect may represent a small storm effect that may not be significant in relation to the other components, particularly at low L values. The reader is reminded that the cutoff times determined in this fashion are initial estimates only. These initial estimates are shown in Table 6 for $1.3 \leq L \leq 1.6$ and Figure 12 for $L = 1.5$.

For the two higher energy channels, it was evident from comparison with the results of Section IV.A. that the electron decay process generally continued beyond the time at which the proton masking level was reached. To refine the cutoff times and to interpolate between the three energy thresholds of the 1963-38C detector, use was made of the fact that the integral spectra must be monotonic and continuous. That

is, a premature cutoff time of some energy would result in a too high natural background that may lead to an unacceptable inversion in the integral spectra at any given time. Iterations were performed on the cutoff times using the condition that the integral spectra must be monotonic and continuous. Since the data from the low energy channel were considered to be more reliable than the data from the higher energy channels, this technique was applied to the 1.2- and 2.4-MeV data only. In view of the inaccuracy of Method 2, two simplifying assumptions were made concerning the data from the low energy channel: (1) the natural background is time independent ($f(t) = 1$ in Equation 2), and (2) for times following the estimated cutoff time, the flux level in quiet periods between storms represents the natural quiet day background. The spectra given by the electron model AE-2 for epoch August 1964 (Vette et al., 1966) was decayed to the date given by the estimated cutoff times to determine if the resulting spectra were monotonic. The decay time model given by Stassinopoulos and Verzariu (1971) was used. Examples of this process are shown in Figures 12 and 13 for $L = 1.5$. In Figure 12 the initial cutoff times estimated from the 1963-38C data are shown together with the final values. At some intermediate point in the iteration many possible lines may be drawn between the points at the grid energies corresponding to the 1963-38C threshold energies. Several of these are indicated in Figure 12. The decayed AE-2 spectra resulting from these curves are indicated in Figure 13 in terms of the AE-2 integral flux. It is clear that the decayed spectrum resulting from lines 3 and 5 in Figure 12 is not an acceptable spectrum, whereas those shown from other combinations are monotonic. However, this process proved to be insufficient in eliminating inversion in the integral spectra entirely. As a test, all available data were processed in this manner, and a three-dimensional model was constructed in which the cutoff time t_c is a continuous function of the variables L and E. Sample calculations were performed with Vette's AE-2 model of the environment (Vette et al., 1966) in which

the effect of cutoff time on orbital flux integrations was investigated. The resulting orbit-integrated spectrum was not monotonic and showed an inversion for energies E > 1.75 MeV.

In order to improve the model and completely eliminate spectral inversions within the energy range 1.00 < E < 3.00 MeV, an iterative technique was devised that, for a given L, would yield approximate boundary values of t_c as a function of energy. The calculation was based on the following inequality, which must hold for all energies between 1 and 3 MeV in the L range of 1.3 < L < 2.0:

$$j_k e^{-\Delta t_k/\tau_k} > j_{k+1} e^{-\Delta t_{k+1}/\tau_{k+1}} \tag{5}$$

where the subscript k refers to a specific energy level, while the k+1 refers to any energy level greater than that of k, τ is the lifetime of the decaying artificial electrons, j is flux, and Δt is the time interval from the data date to an arbitrary decay date. The fluxes are taken as input for a given epoch. Then this inequality defines conditions on the Δt's that set limits on the cutoff dates.

For integral spectra, by definition

$$j_k \geq j_{k+1}$$

and according to the decay time model of Stassinopoulos and Verzariu

$$\tau_k > \tau_{k+1}$$

and consequently, from Equation 5, when replacing Δt with the cutoff time t_c minus the data time t_d, one obtains:

$$(t_c)_{k+1} > \tau_{k+1} \ln\left(\frac{j_{k+1}}{j_k}\right) + \frac{\tau_{k+1}}{\tau_k}(t_c)_k + t_d\left(1 - \frac{\tau_{k+1}}{\tau_k}\right) \tag{6}$$

For a fixed value of t_d (752 days for the AE-2) and for given t_c, τ, and j at some arbitrary energy k, a lower bound for the cutoff time at some other arbitrary k + 1 can be determined from the Equation 6. A refined set of cutoff times was thus obtained for each L value. In order to assume a linear relationship between cutoff times and energy, the total energy range (0.25 < E < 3.0 MeV) was divided into five sections small enough to assure that the partial derivatives of t_c were constant within each. The final linearized cutoff times for every L value are shown in Figure 14 over the entire energy range considered. In addition, the final cutoff time for L = 1.5 is compared with the initial estimates of Figure 12. Table 7 gives t_c at selected energy thresholds as month and year after Starfish injection.

The continuous functional relationship of t_c to its variables L and E is given by

$$t_c = \alpha EL + \beta E + \gamma L + \delta \qquad (7)$$

where the coefficients were obtained by linear curve fitting.

Because of the accuracy of the method, no dependence of t_c on B has been considered in Method 2 as with Method 1. The coefficients of Equation 7 are presented in Table 8. It is estimated that the maximum error in the cutoff times given by Equation 7 due to any cause does not exceed 15%.

C. The Cutoff Time Model

The comparison of the results of Methods 1 and 2 are presented in Figures 15 through 22. The cutoff times, with units of months after Starfish injection, are shown as a function of energy for L values in the range $1.3 \leq L \leq 2.0$. In general it can be seen that Method 1 provides better coverage at low energies, and Method 2 provides better

coverage at high energies. The values presented for Method 2 are obtained by interpolation between the three energy thresholds of the 1963-38C satellite as described in Section IV.B. For Method 1 the values are presented at thresholds corresponding to the lower energy limit of each channel of the OGO spectrometer. In the regions where the results of the two methods overlap, it is clear that the cutoff times agree within the estimated error. The estimated error for the Method 2 results corresponds to the maximum figure of 15% discussed in Section IV.B. The most significant differences between the two methods occur at low L values and high energies, the greatest difference being approximately 18 months at L = 1.3 and E = 2 MeV.

The accuracy of both methods presented is likely to be poor in the regions where extrapolations are performed. These regions are at high energies for Method 2, where extrapolations beyond the proton background have been performed, and at high energies and low L values for Method 1, where cutoff times later than the data epoch have been obtained by extrapolating for the quiet day natural background. The maximum difference between the results of the two methods quoted in the previous paragraph occurs in a region where both methods are extrapolating.

Improved estimates of the cutoff times in these extrapolation regions can be obtained by comparing conditions before Starfish injection with those at epochs later than the cutoff times. Estimates of the high-energy electron flux for pre-Starfish epochs can be obtained using proton data from Explorer 4 (McIlwain, 1963; Vette, 1966) for epoch 1958 and Explorer 12 (Ackerson and Frank, 1966) for epoch 1961. Both satellites measured total particle omnidirectional fluxes, and the energy thresholds for electrons and protons are shown in Table 1. Assuming that the observed count rate from these satellites resulted

entirely from electrons, an upper limit can be obtained for the pre-Starfish electron fluxes above 1.6 and 2 MeV. (Note that it is probable that less than 60% of the total count rate actually resulted from electrons.) The equatorial omnidirectional flux radial profiles are shown in Figure 23 for data from these two satellites. For Explorer 4, the data have been extrapolated to the equator using the B dependence given by the proton model AP-4 (Vette, 1966). Shown also in Figure 23 are the AE-5 electron radial profiles (Teague and Vette, 1972) for epoch October 1967 corresponding to 63 months after Starfish injection. If it is assumed that the broken curves in Figure 23 represent the natural electron flux following the completion of the Starfish decay process, estimates can be made of the cutoff times for the low L values at which Method 1 extrapolated for the natural electron flux. Using the decay time model presented in Section III, the cutoff times shown in Table 9 are obtained. These values are compared with those given by Methods 1 and 2, and it is clearly evident that in this region where both models are extrapolating, the results of Method 2 are superior.

In determining the final cutoff time model on the basis of the results of Methods 1 and 2, emphasis was given to Method 2 for high energies and low L values. The final cutoff time model is shown in Figures 15 through 22 as solid lines. A threshold-energy vs L-value map for cutoff times is presented in Figure 24 summarizing the model. The dotted curve in this figure represents the latest epoch for which data were available for Method 1. Estimates of the errors associated with the cutoff time model are presented in Table 10 for various L values and energies. It is clear from Figure 24 that the longest-lived particles from Starfish occur at $L \simeq 1.3$ earth radii and $E_T \simeq 1.6$ MeV, and that these particles are significant in relation to the natural content of the belt for approximately 8 years after Starfish injection. However, it is also clear from Table 10 that the maximum lifetime coincides with maximum error for the reasons discussed in this section.

Qualitative confirmation of the cutoff time model can be obtained by comparison of the model with data from the OV3-3 and OGO 5 data. The energies of electrons detected by the spectrometers on these satellites are given in Table 1. Note that only the high-energy channels from OGO 5 are used in this study and that the spectrometer measured fluxes in four additional lower energy channels. Figures 25 through 28 show the residual Starfish flux component for energies $E_T > 500$ keV for $1.6 \geq L \geq 1.3$. Equatorial perpendicular integral flux spectra are shown for 48 and 72 months after Starfish injection (m.a.s.) and correspond to epochs of mid-1966 and mid-1968. Integral flux data are shown from the OGO 3 and OV3-3 satellites for epoch mid-1966 and from the OGO 5 satellite for epoch 1968. Note that, although storm effects are generally small at these L values, only quiet time data has been used. It is evident from Table 1 that the energy ranges covered by the OGO 5 spectrometer are not contiguous. Estimates of the integral fluxes were made by using linear interpolation on the logarithm of the differential fluxes. In Table 1, it can be seen that the OV3-3 spectrometer measured electrons with $E < 2.472$ MeV only. For $L = 1.3$ and 1.4, the differential spectra given by the OV3-3 data are very hard, and significant error is introduced in the integral spectra if the flux of particles with $E > 2.472$ MeV is assumed to be zero. Estimates of this part of the spectrum were made by using linear interpolation on the logarithm of the flux with the boundary condition that the logarithm of the flux for $E > 4$ MeV was zero. In comparing the data and the model it should be noted that the model is an estimate of the residual Starfish flux component, whereas the data correspond to total (i.e., Starfish plus natural) flux. Thus, if the model is a good representation of the data, it may be inferred that the Starfish component is dominant and that the cutoff time should be appreciably later than the epoch of the data. Conversely, if the observed fluxes are clearly greater than the model, then the Starfish component has become insignificant and the cutoff time should be earlier than the

data epoch. The model cutoff times are indicated on the abcissa scale of each of the Figures 25 through 28. As discussed previously, it should be appreciated that a significant error is associated with the model curves, and differences of less than a factor of two between the model and the data may not be significant. For L = 1.3 (Figure 25), the model is a good representation of the data at both epochs with the possible exception of the 637-keV, OGO 5 data point, and thus, the cutoff times should be at epochs greater than T_S = 72 m.a.s. From the cutoff time scale, this can be seen to be so with the exception of the lower energies where cutoff is given as $t_c \sim 71$ m.a.s. The same observations may be made at L = 1.4, except that the 637-keV data value now lies clearly above the model curve. At L = 1.5, the highest energy channel of the OGO 5 spectrometer is clearly above the model and indicates that cutoff has been passed for these energies. For the highest L value shown, the model is significantly below the OGO 5 data for all energies, indicating that cutoff occurred for $T_S < 72$ m.a.s. However, the model is a good representation of the OV3-3 and OGO 3 data for T_S = 48 m.a.s., indicating that $t_c > 48$ m.a.s. It can be seen from the t_c scale on Figure 28 that the cutoff time model exhibits these characteristics.

Approximate estimates of the natural high-energy flux at low L values may be obtained by decaying the Starfish model to $t = t_c$. These estimates are shown in Figures 25 through 28 as broken lines. It should be emphasized that an error of a factor of three is likely on these fluxes, except in regions where direct comparison can be made with the OGO 5 data (i.e., L = 1.6).

Page intentionally left blank

Page intentionally left blank

V. CONCLUSIONS

A model of the inner zone residual Starfish flux component in September 1964 has been presented, indicating that the most significant residuals in relation to the natural background remain at low L values and intermediate energies (approximately 0.5 MeV). A more complete description of the derivation of the Starfish flux model was previously presented by Teague and Vette (1972). An average decay time model has been presented for $0.1 \leq E \leq 3.0$ MeV based upon data from the OGO 1, OGO 3, Explorer 26, Pegasus A and B, Explorer 15, and OV1-2 satellites and the Stassinopoulos and Verzariu decay time model. Considerable differences are observed between the various decay time values, particularly for energies $E < 500$ keV. The average decay time model indicates that a maximum decay time at any L value occurs in the energy range of $0.3 \leq E < 1$ MeV. The model estimates the maximum decay time in the inner zone to be 380 days approximately at $E = 1$ MeV and $L = 1.45$. The Starfish flux and decay time models have been used to show substantial agreement with the OGO 1 and 3 and 1963-38C data in January 1965 and June 1966.

Estimates have been made of the times at which the Starfish decay process can be considered to be completed, that is, when the natural electron content of the inner zone is comparable to the residual Starfish flux. These estimates have been made by two separate methods, and substantial agreement between the results have been demonstrated. Qualitative confirmation of the cutoff times has been obtained by comparison of the Starfish model and data from the OV3-3 and OGO 5 satellites. The cutoff time model indicates that the Starfish electrons are longest lived in the inner zone at $L = 1.3$ and $E = 1.6$ MeV approximately

and reach the natural background approximately 8 years (July 1970) after Starfish injection. Therefore, an important conclusion of the present analysis is that, for present epochs, the Starfish nuclear explosion no longer affects the trapped particles in the radiation zones.

REFERENCES

Ackerson, K. L., and L. A. Frank, "Explorer 12 Observations of Charged Particles in The Inner Radiation Zone," University of Iowa, 66-13, 1966.

Beall, D. S., "Graphs of Selected Data from Satellite 1963-38C," Applied Physics Laboratory, TG 1050-1 through TG 1050-5, 1969.

Brown, W. L., "Observations of the Transient Behavior of Electrons in the Artificial Radiation Belts," Radiation Trapped in the Earth's Magnetic Field, B. M. McCormac, ed., Gordon and Breach, 1965.

Farley, T. A., "Radial Diffusion of Starfish Electrons," J. Geophys. Res., 74(14), 3591-3600, 1969.

McIlwain, C. E., "Coordinates for Mapping the Distribution of Magnetically Trapped Particles," J. Geophys. Res., 66, 3681-4078, 1963.

Pfitzer, K. A., "An Experimental Study of Electron Fluxes from 50 keV to 4 MeV in the Inner Radiation Belt," University of Minnesota, Technical Report CR-123, Aug. 1968.

Rosen, A., and N. L. Sanders, "Loss and Replenishment of Electrons in the Inner Radiation Zone during 1965-1967, J. Geophys. Res., 76(1), 110-121, 1971.

Stassinopoulos, E. G., and P. Verzariu, "General Formula for Decay Lifetimes of Starfish Electrons," J. Geophys. Res., 76(7), 1841-1844, 1971.

Teague, M. J., and J. I. Vette, "The Inner Zone Electron Model AE-5," NSSDC 72-10, Sept. 1972.

Teague, M. J., "The Calibration Constants for the OGO 1/3 Electron Spectrometer," NSSDC 70-14, Oct. 1970.

Vampola, A. L., "Energetic Electrons at Latitudes above the Outer Zone Cutoff," J. Geophys. Res., 74(5), 1254-1269, 1969.

Vampola, A. L., Private Communication, Dec. 1972.

Vette, J. I., "Models of the Trapped Radiation Environment Volume I: Inner Zone Protons and Electrons," NASA SP-3024, 1966.

West, H. I., Jr., J. H. Wujack, J. H. McQuaid, N. C. Jensen, R. G. D'Arcy, Jr., R. W. Hill, and R. M. Bogdanowicz, "The LRL Electron and Proton Spectrometer on NASA's Orbiting Geophysical Observatory V(E) (Instrumentation and Calibration)" UCRL-50572, June 2, 1969.

Page intentionally left blank

Page intentionally left blank

TABLE 1. Energy Ranges of Data Sets

Satellite	Channel	Electron Energy Range (keV)	Type of Measurement
OGO 1 and 3	1	36 - 133	Unidirectional Differential Electron Flux
	2	133 - 292	
	3	292 - 690	September 1964 to April 1965 (OGO 1)
	4	690 - 1970	June 1966 to December 1967 (OGO 3)
	5	1970 - 4740	
OV3-3	1	2147 - 2472	Unidirectional Differential Electron Flux
	2	1880 - 2200	
	3	1615 - 1925	August to December 1966
	4	1329 - 1651	
	5	1075 - 1375	
	6	814.5 - 1099.5	
	7	574.5 - 849.5	
	8	350 - 600	
	9	225 - 375	
OGO 5	5	637 - 1007	Unidirectional Differential Electron Flux
	6	270 - 1790	
	7	2550 - 3090	1968
Explorer 4		>2000	Omnidirectional Integral Total Particle Flux
			Protons E > 43 MeV
Explorer 12		>1600	Omnidirectional Integral Total Particle Flux
			Proton E > 21 MeV

TABLE 2. Polynomial Coefficients for Starfish Flux Model

	133 - 292 keV					292 - 690 keV					690 - 1970 keV					1970 - 4740 keV				
L	a_0	$a_1 \times 10^3$	$a_2 \times 10^4$	$a_3 \times 10^5$	θ	a_0	$a_1 \times 10^3$	$a_2 \times 10^4$	$a_3 \times 10^5$	θ	a_0	$a_1 \times 10^3$	$a_2 \times 10^4$	$a_3 \times 10^5$	θ	a_0	$a_1 \times 10^3$	$a_2 \times 10^4$	$a_3 \times 10^5$	θ
1.3	4.613	-11.94	-1.406	-3.291	75	4.447	-21.67	-1.007	-4.950	74	3.75	-41.4	11.9	-11.8	72.5	3.057	-32.00	.7505	-5.181	72.5
1.4	4.895	-25.68	-1.136	-2.656	71	4.529	2.770	-22.14	0	67.5	3.819	-22.14	-2.603	-.5512	70	3.182	-24.37	-.7157	-3.214	72.5
1.5	4.959	.4001	-5.455	0	77.5	4.622	-20.38	5.598	-5.702	66	3.750	-14.46	-13.44	0	67	2.857	-14.33	-3.551	-.6104	74.5
1.6	4.989	-7.791	3.874	-2.032	74	4.549	-22.23	-2.539	-1.328	64.5	3.494	-9.510	-9.798	0	67	2.321	-15.69	-5.382	-.4008	67
1.7	5.004	-13.06	1.852	-1.063	75	4.412	-18.90	-5.672	-.6142	63.5	3.037	-5.956	-9.806	0	66					
1.8	4.951	-15.28	-3.408	-.3547	65	4.250	-22.19	-6.253	.1122	60.5	2.629	-16.67	-5.856	-.0271	65					
1.9	4.913	1.128	-8.49	0	70	4.033	-11.82	-2.910	-1.070	63.5	2.255	-16.59	-6.773	.4596	65	NO DATA				
2.0	4.839	-7.729	1.624	-.8415	79	3.792	-18.58	7.626	-1.882	75	1.998	-16.32	-5.651	-.4836	65					
2.2	4.586	-2.266	-2.219	-.4664	70	3.29	-4.455	-1.576	-.2088	80	NO DATA									

Coefficients provide flux in units of electrons/cm^2 sec ster keV at epoch September 1964.

TABLE 3. OGO BASED STARFISH DECAY TIMES*

	Energy Ranges (keV)			
L	133 - 292	292 - 690	690 - 1970	1970 - 4740
1.4	163 ± 60	216 ± 70	380 ± 20	310 ± 20
1.5	200 ± 70	230 ± 70	375 ± 20	310 ± 20
1.6	233 ± 45	260 ± 50	312 ± 20	290 ± 20
1.7	265 ± 42	230 ± 42	310 ± 40	ND**
1.8	267 ± 37	230 ± 37	ND**	ND**
1.9	250 ± 30	211 ± 30	ND**	ND**
2.0	219 ± 30	150 ± 25	ND**	ND**
2.2	98 ± 30	103 ± 25	ND**	ND**

*Decay times in days.
**ND denotes no data.

TABLE 4. COMPARISON OF INTEGRAL FLUX DECAY TIMES*

	Energy Threshold (keV)						
	>133	>292		>690		>1970	
L	OGO	OGO	S and V**	OGO	S and V**	OGO	S and V**
1.3	ND***	ND***	382 - 333	ND***	368 - 317	ND***	325 - 265
1.4	230 ± 60	265 ± 70	415	348 ± 20	390	310 ± 20	340
1.5	245 ± 60	280 ± 70	445	350 ± 20	410	310 ± 20	320
1.6	256 ± 45	270 ± 45	445	305 ± 20	400	290 ± 20	270
1.7	240 ± 42	240 ± 42	420	310 ± 40	360	ND***	180
1.8	250 ± 37	230 ± 37	360	ND***	300	ND***	80
1.9	240 ± 30	211 ± 30	290	ND***	215	ND***	7.6
2.0	200 ± 30	150 ± 25	200	ND***	135	ND***	ND***
2.2	100 ± 30	103 ± 25	64	ND***	15	ND***	ND***

*Decay times in days.
**Stassinopoulos and Verzariu.
***ND denotes no data.

TABLE 5. CUTOFF TIMES* METHOD 1

Energy Threshold (keV)														
>36			>133		>292			>690			>1970			
L	a**	b***	a**	b***	a**	b***	c+	a**	b***	c+	a**	b***	c+	
1.3	ND++	8/65 (37 ±4)	ND++	11/65 (40 ±4)	ND++	11/66 (52 ±4)	4/67 (57)	ND++	12/68 (77 ±5)	2/69 (79)	ND++	12/68 (77 ±6)	12/68 (77)	
1.4	9/65 (38)	11/65 (40 ±3)	10/65 (39)	1/66 (42 ±3)	7/66 (48)	9/66 (50 ±3)	2/67 (55)	4/68 (69)	6/68 (71 ±4)	9/68 (74)	2/68 (67)	6/68 (71 ±4)	6/68 (71)	
1.5	7/65 (36)	8/65 (37 ±3)	9/65 (38)	10/65 (39 ±3)	6/66 (47)	8/66 (49 ±3)	12/66 (53)	8/67 (61)	10/67 (63 ±4)	2/68 (67)	3/67 (56)	4/67 (57 ±4)	4/67 (57)	
1.6	5/65 (34)	6/65 (35 ±2)	7/65 (36)	8/65 (37 ±2)	5/66 (46)	7/66 (48 ±3)	11/66 (52)	8/66 (49)	11/66 (52 ±4)	2/67 (55)	6/66 (47)	4/66 (45 ±4)	4/66 (45)	
1.7	3/65 (32)	3/65 (32 ±2)	6/65 (35)	6/65 (35 ±2)	1/66 (42)	1/66 (43 ±3)	7/66 (48)	9/65 (38)	10/65 (39 ±4)	11/65 (40)	ND++	ND++	ND++	
1.8	12/64 (29)	1/65 (30 ±2)	5/65 (34)	5/65 (34 ±2)	8/65 (37)	9/65 (38 ±2)	12/65 (41)	ND++	ND++	ND++	ND++	ND++	ND++	
1.9	9/64 (26) or		3/65 (32)	3/65 (32 ±2)	4/65 (33)	5/65 (34 ±2)	6/65 (35)	ND++	ND++	ND++	ND++	ND++	ND++	
2.0	earlier		2/65 (31)	2/65 (31 ±2)	ND++	ND++	ND++	ND++	ND++	ND++	ND++	ND++	ND++	
2.2			10/64 (27)	10/64 (27 ±2)	ND++	ND++	ND++	ND++	ND++	ND++	ND++	ND++	ND++	

*Cutoff times in month and year (months after Starfish injection).
**a OGO decay times.
***b Present model.
+c Stassinopoulos and Verzariu model.
++ND denotes no data.

TABLE 6. INITIAL CUTOFF TIME* ESTIMATES METHOD 2

	Energy Threshold (MeV)		
L	.28	1.2	2.4
1.3	54	47	21
1.4	51	71	15
1.5	47	61	12
1.6	43	51	9

*Cutoff times in months after Starfish injection.

TABLE 7. FINAL CUTOFF TIMES* METHOD 2

	Energy Threshold (MeV)					
L	.25	.75	1.0	1.5	2.0	3.0
1.3	1/67 (54)	5/69 (82)	2/70 (91)	8/70 (97)	6/70 (95)	11/69 (88)
1.4	9/66 (50)	8/68 (73)	3/69 (80)	6/69 (83)	3/69 (80)	4/68 (69)
1.5	5/66 (46)	11/67 (64)	3/68 (68)	3/68 (68)	10/67 (63)	10/66 (51)
1.6	1/66 (42)	2/67 (55)	4/67 (57)	1/67 (54)	6/66 (47)	3/65 (32)
1.7	10/65 (39)	4/66 (45)	5/66 (46)	10/65 (39)	2/65 (31)	8/63 (13)
1.8	6/65 (35)	7/65 (36)	6/65 (35)	8/64 (25)	10/63 (15)	ND**
1.9	3/65 (32)	10/64 (27)	6/64 (23)	4/63 (9)	ND**	ND**
2.0	11/64 (28)	1/64 (18)	7/63 (12)	ND**	ND**	ND**
2.1	7/64 (24)	4/63 (9)	8/62 (1)	ND**	ND**	ND**

*Cutoff times in month and year (months after Starfish injection); estimated error < 15%.
**ND denotes no data.

TABLE 8. CUTOFF TIME COEFFICIENTS*

Energy Range (MeV)	L Range (earth radii)	α	β	γ	δ
0.10 - 0.15	<1.4	-314.0	493.4	54.0	-38.72
0.15 - 0.20	<1.4	-48.0	121.0	-18.97	63.43
0.20 - 0.30	<1.4	-64.67	144.33	-16.42	59.83
0.10 - 0.15	≥ 1.4	-48.0	121.0	-18.97	63.43
0.15 - 0.20	≥ 1.4	-64.67	144.33	-16.42	59.83
0.20 - 0.30	≥ 1.4	-105.83	201.67	-8.29	48.58
0.30 - 0.40	ALL	-135.71	249.43	.7142	34.171
0.40 - 0.55	ALL	-128.57	233.14	-2.143	40.687
0.55 - 0.75	ALL	-117.87	208.73	-8.031	54.113
0.75 - 0.90	ALL	-93.324	164.65	-26.437	87.175
0.90 - 1.0	ALL	-72.714	121.43	-44.986	126.07
1.0 - 1.1	ALL	-29.357	48.215	-91.279	204.11
1.1 - 1.25	ALL	-47.304	74.827	-71.537	174.83
1.25 - 1.5	ALL	-35.332	52.132	-86.502	203.20
1.5 - 1.7	ALL	-20.667	27.867	-108.50	239.60
1.7 - 2.0	ALL	-20.001	23.344	-110.65	248.68
2.0 - 3.0	ALL	-14.530	12.790	-121.61	269.79

*$t_c = \alpha EL + \beta E + \gamma L + \delta$ months.

TABLE 9. Cutoff Times* Using Explorer 12 and Explorer 4 Data

L	Energy (MeV)					
	1.6			2.0		
Value	Explorer Data	Method 1	Method 2	Explorer Data	Method 1	Method 2
1.3	94	77	97	103	77	95
1.4	90	71	83	90	71	80
1.5	82	60	68	83	57	63

*Cutoff times in months after Starfish injection.

TABLE 10. ACCURACY OF CUTOFF TIME* MODEL

	Energy (MeV)						
L	.03	.05	.1	.3	.5	1	3
1.3	±4	±4	±4	±4	±5	±8	±10
1.4	±3	±3	±3	±3	±4	±8	±10
1.5	±3	±3	±3	±3	±4	±8	±10
1.6	±3	±3	±3	±3	±4	±6	±7
1.7	±3	±3	±3	±3	±4	±8	±8
1.8	±3	±3	±3	±3	±6	±8	
1.9	±8	±7	±5	±5	±7	±8	
2	±8	±7	±5	±6	±8	±9	

*Cutoff time in months after Starfish injection.

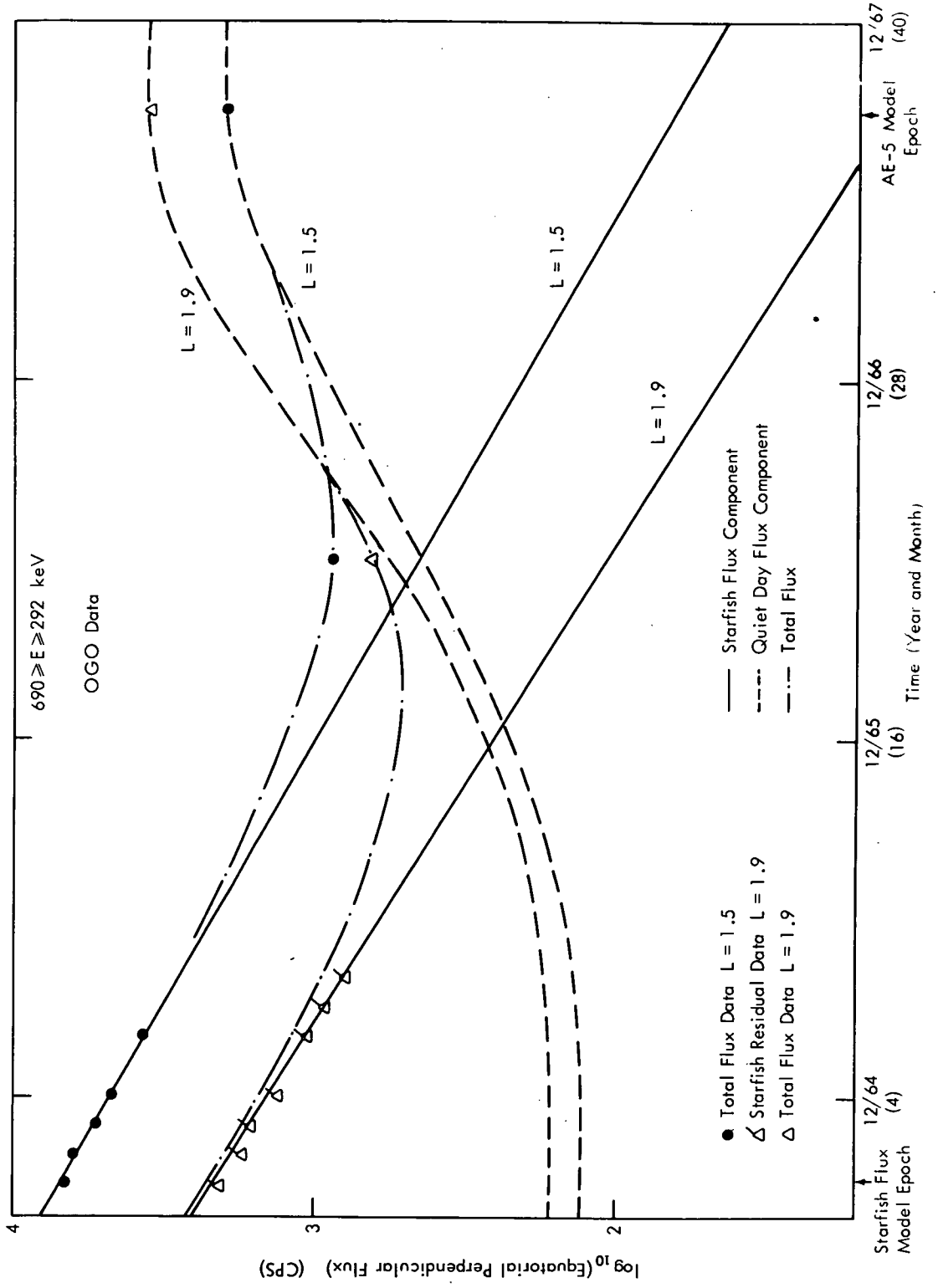

Figure 1. Separation of Flux Components

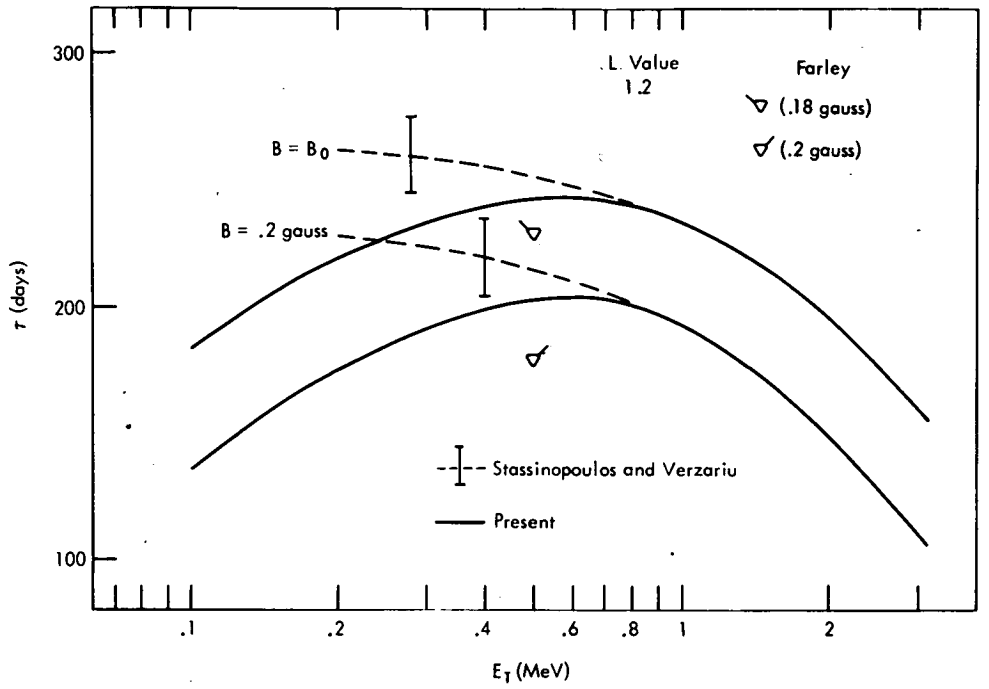

Figure 2. The Decay Time Model

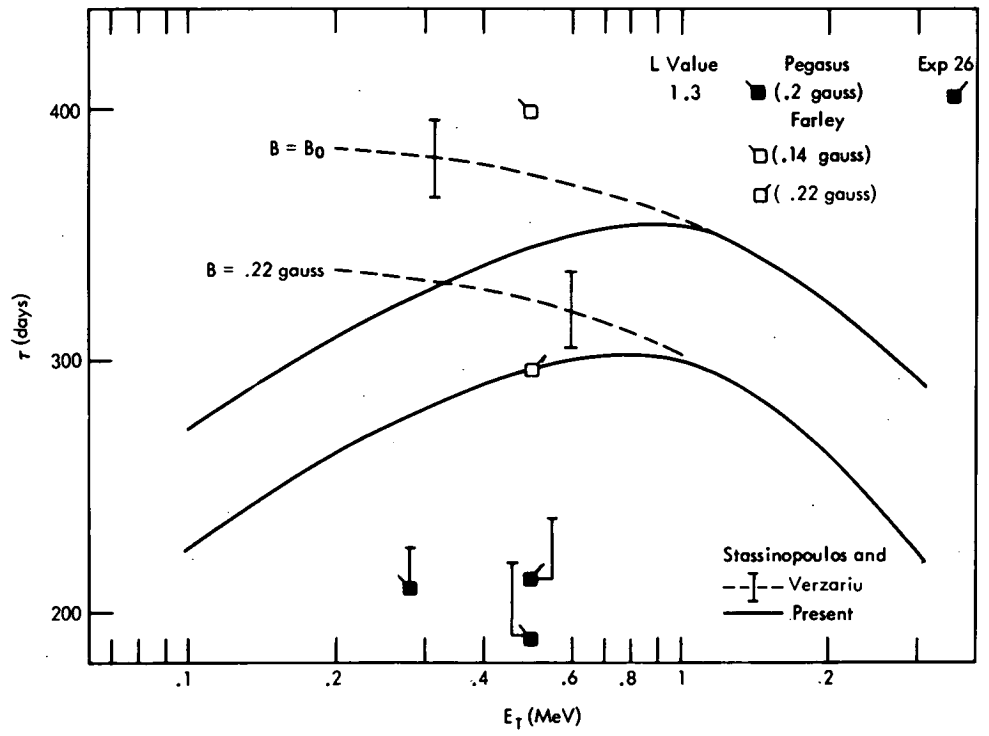

Figure 3. The Decay Time Model

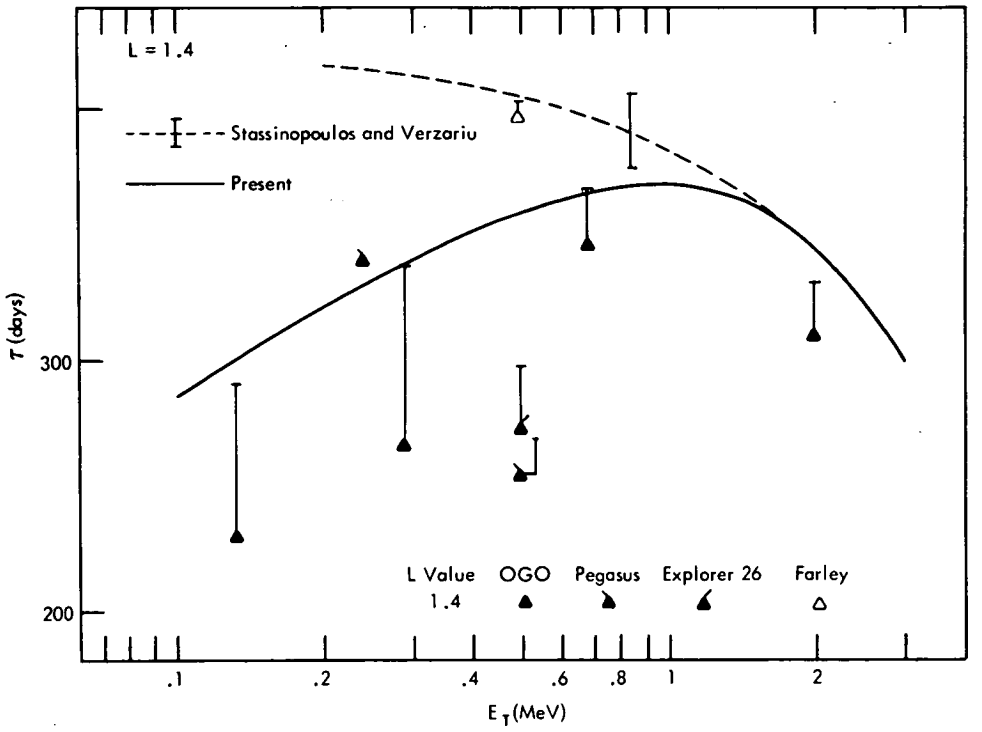

Figure 4. The Decay Time Model

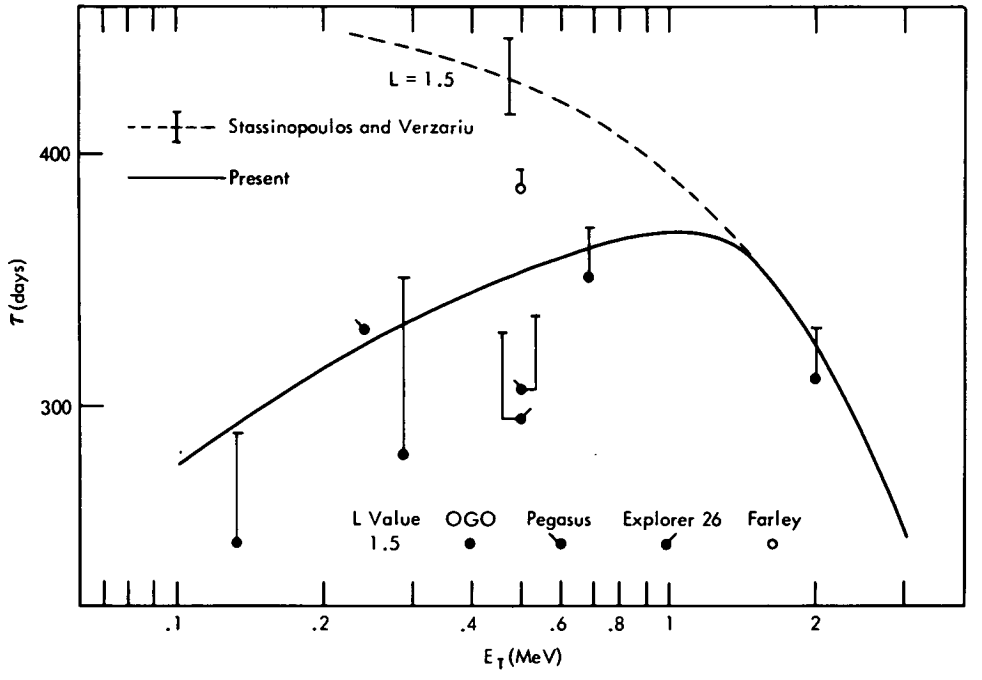

Figure 5. The Decay Time Model

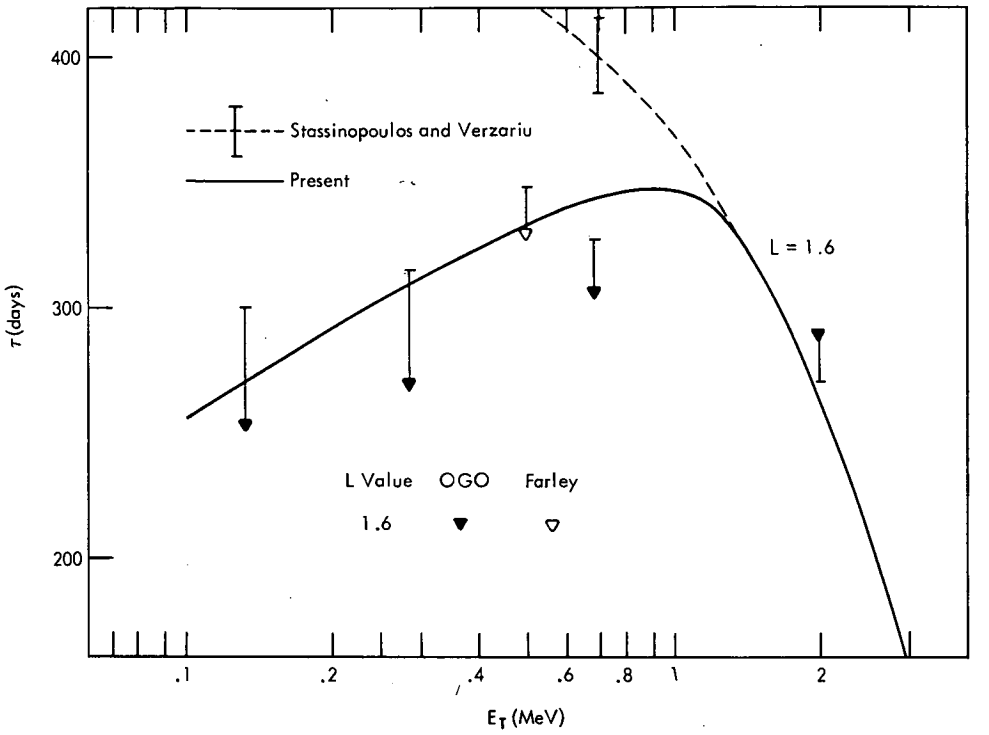

Figure 6. The Decay Time Model

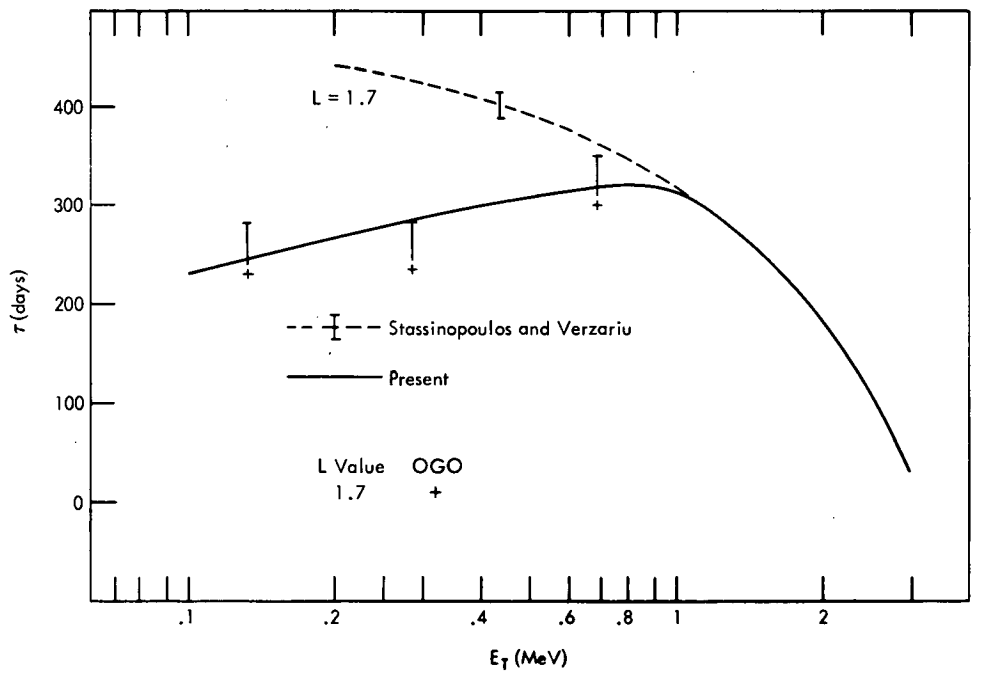

Figure 7. The Decay Time Model

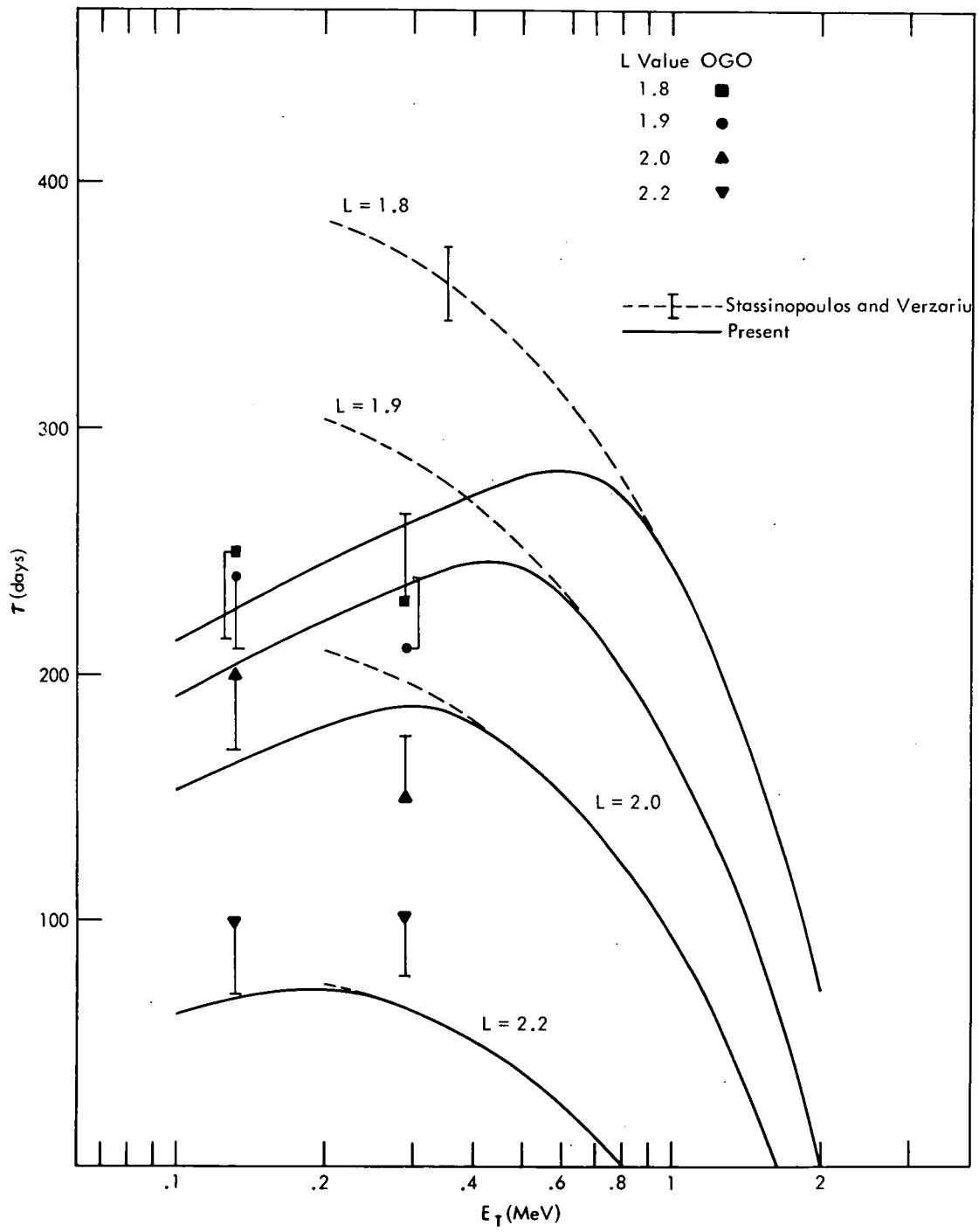

Figure 8. The Decay Time Model

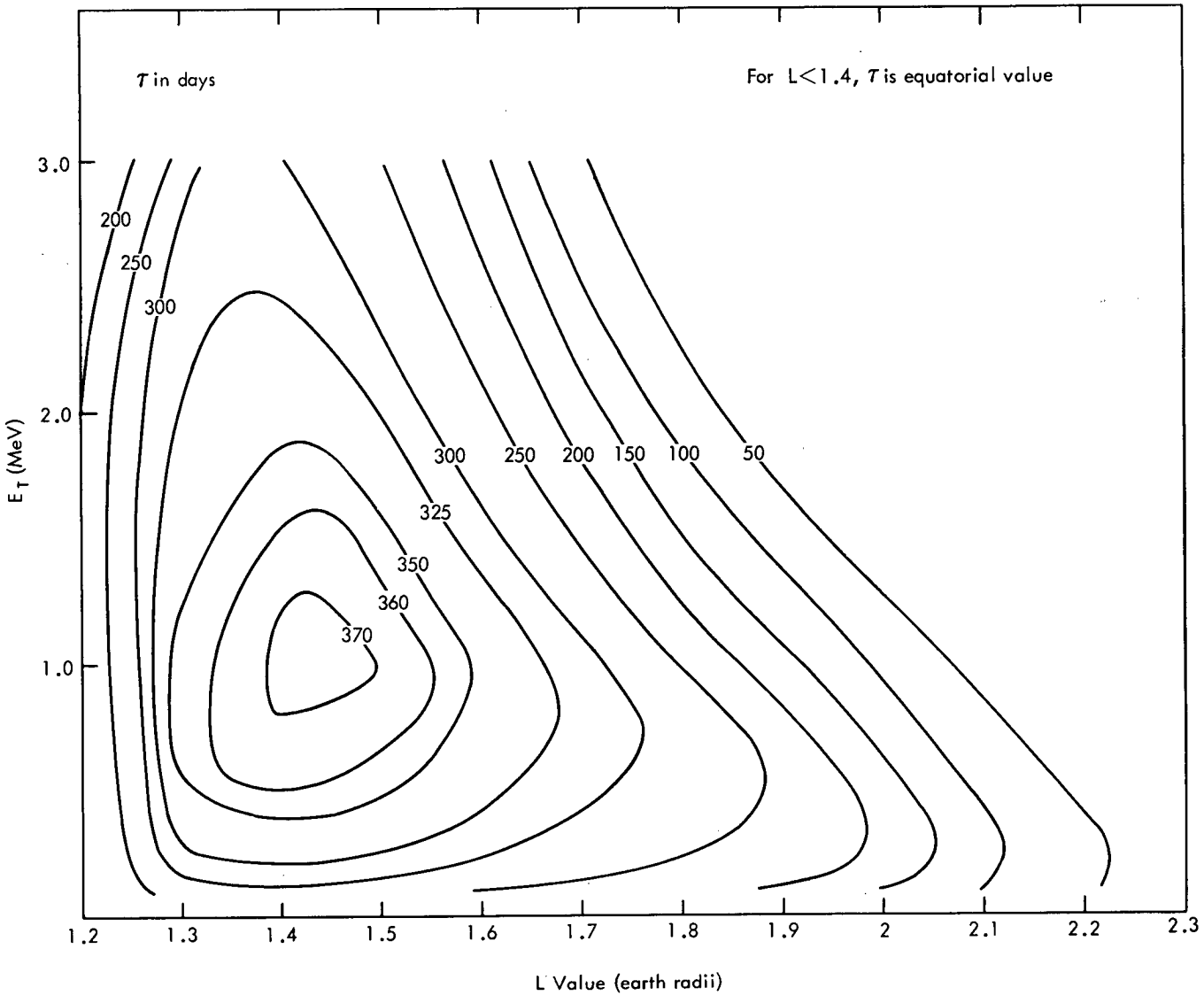

Figure 9. Constant Decay Time Contours

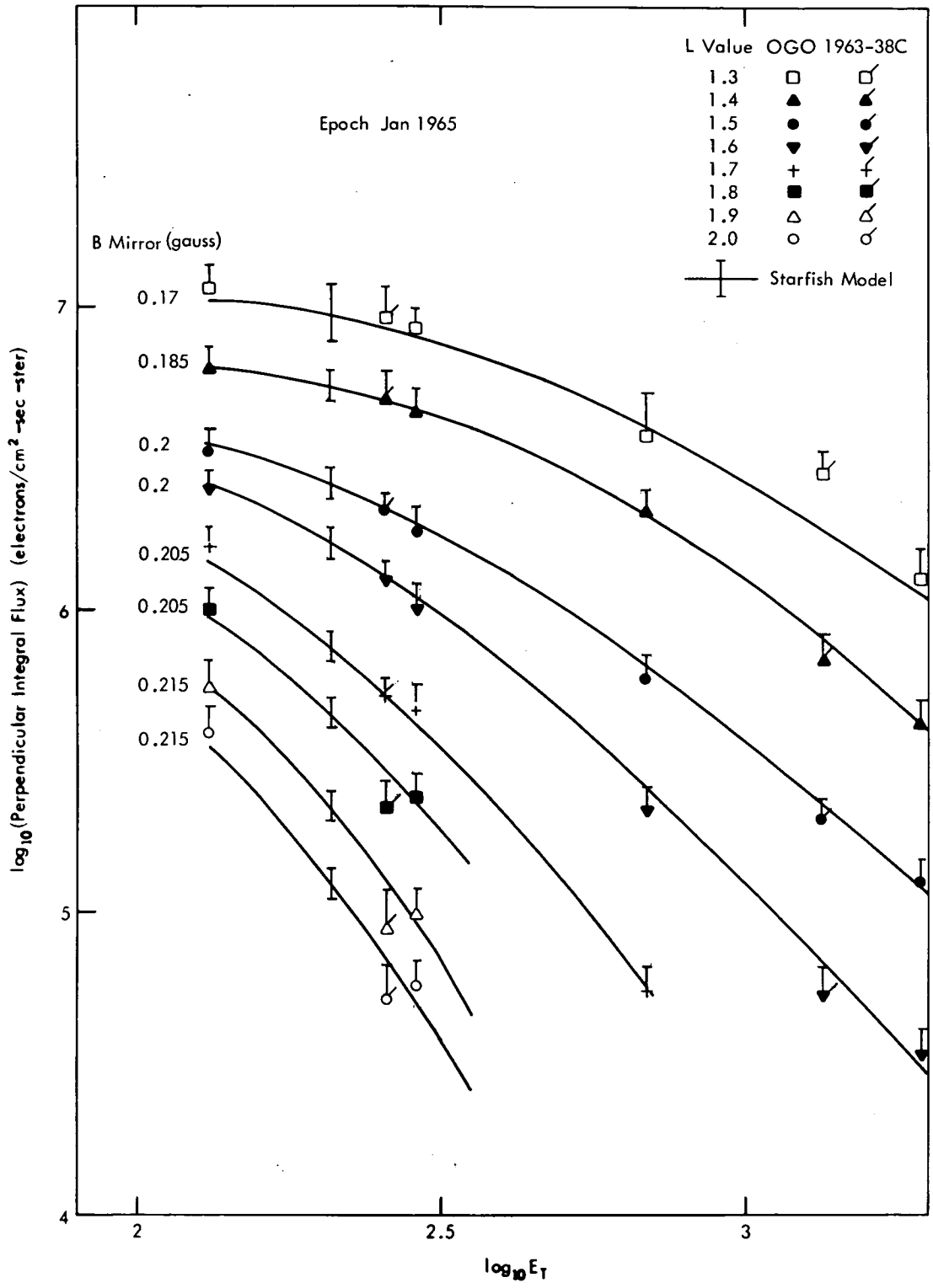

Figure 10. Comparison of the Starfish Model and the 1963-38C Data

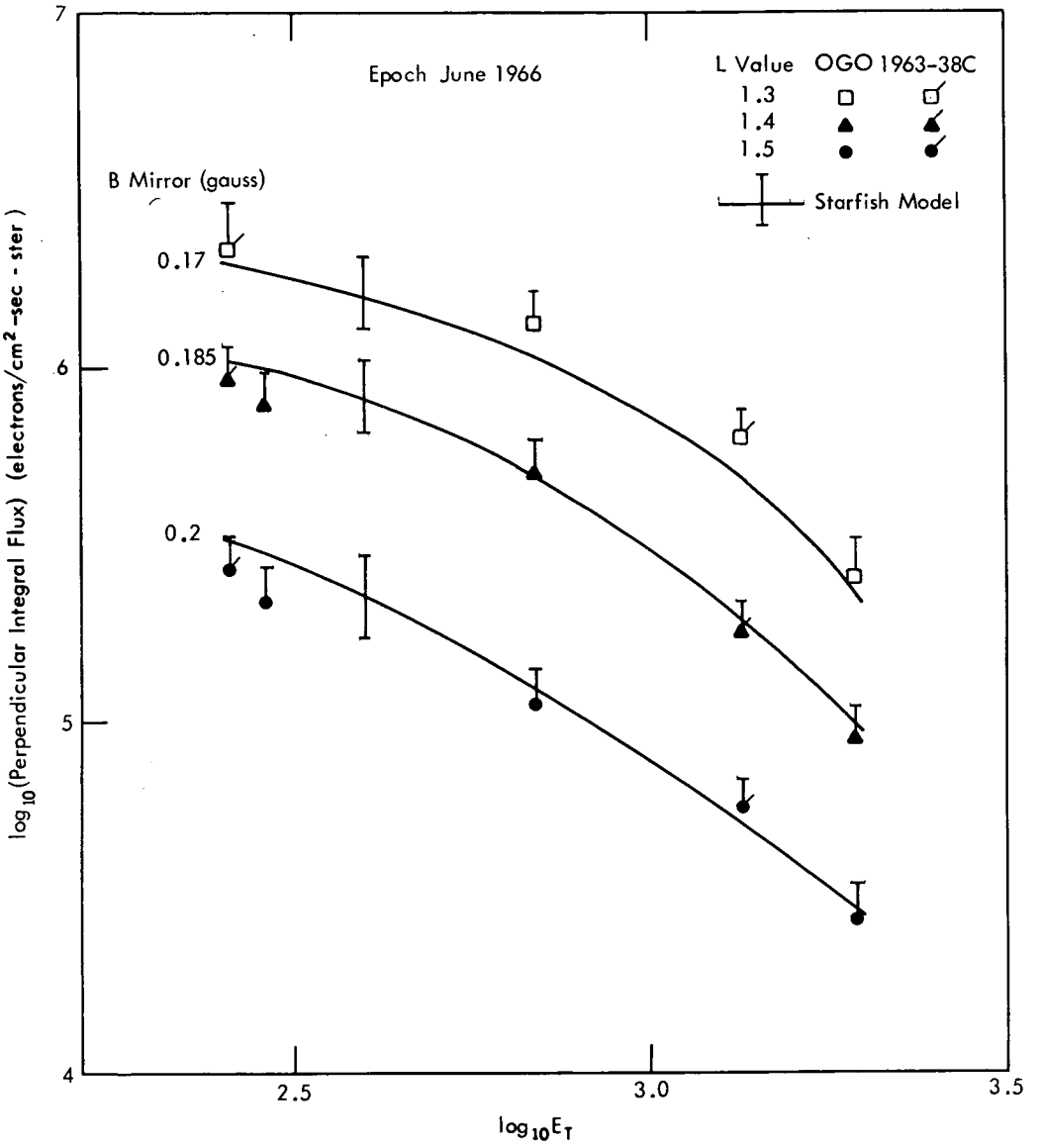

Figure 11. Comparison of the Starfish Model and the 1963-38C Data

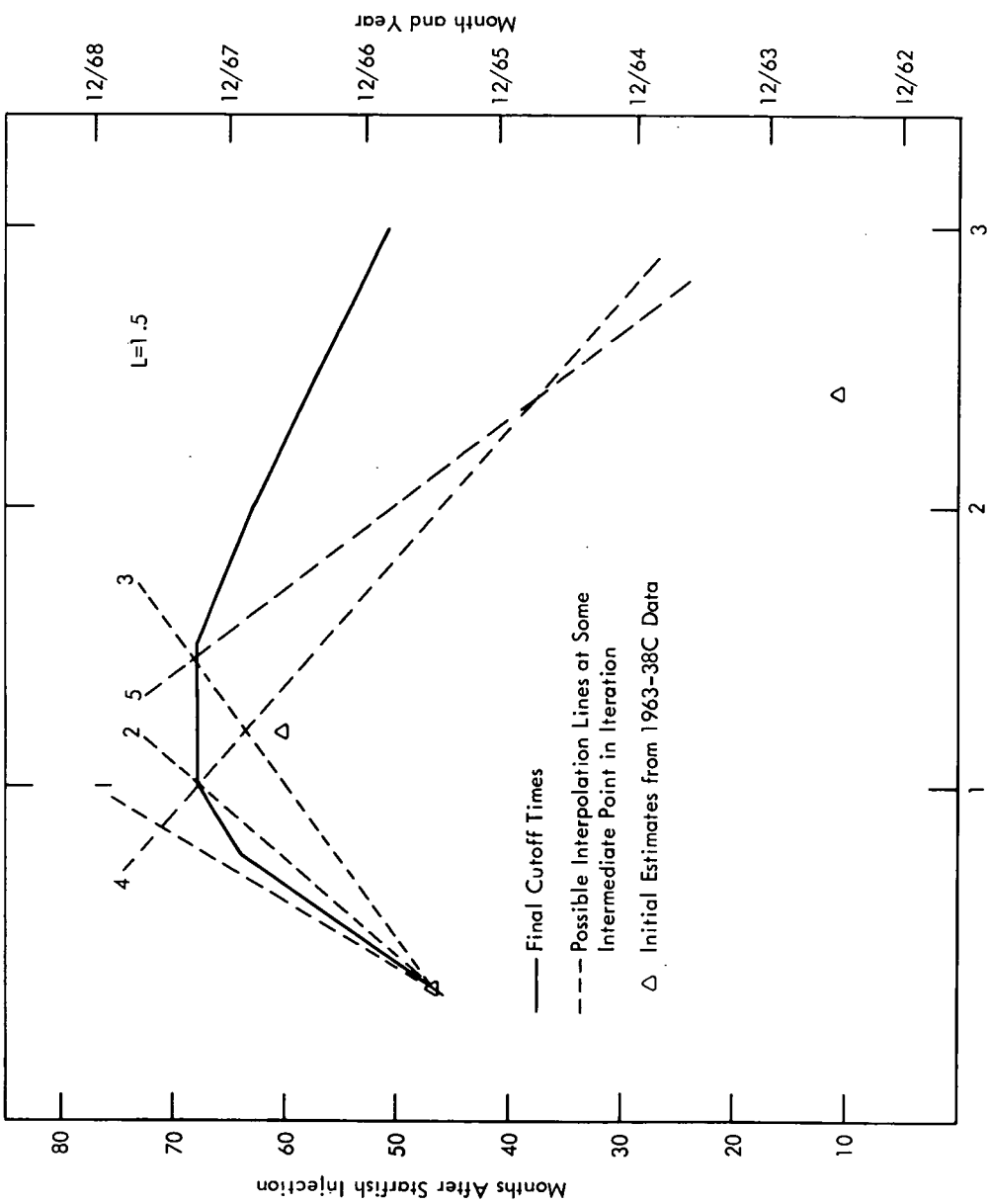

Figure 12. Cutoff Times for L = 1.5

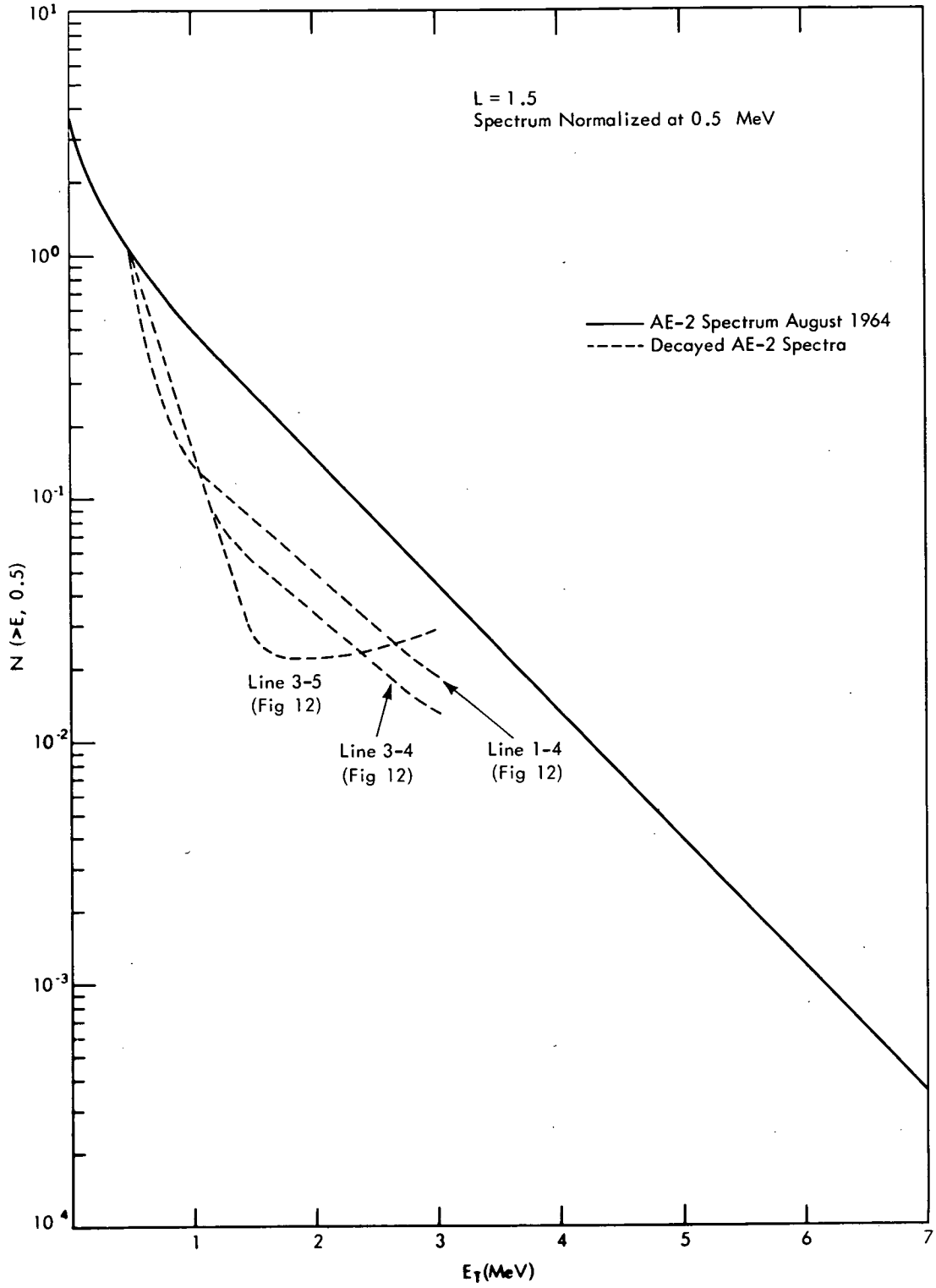

Figure 13. Decay of the AE-2 Spectrum

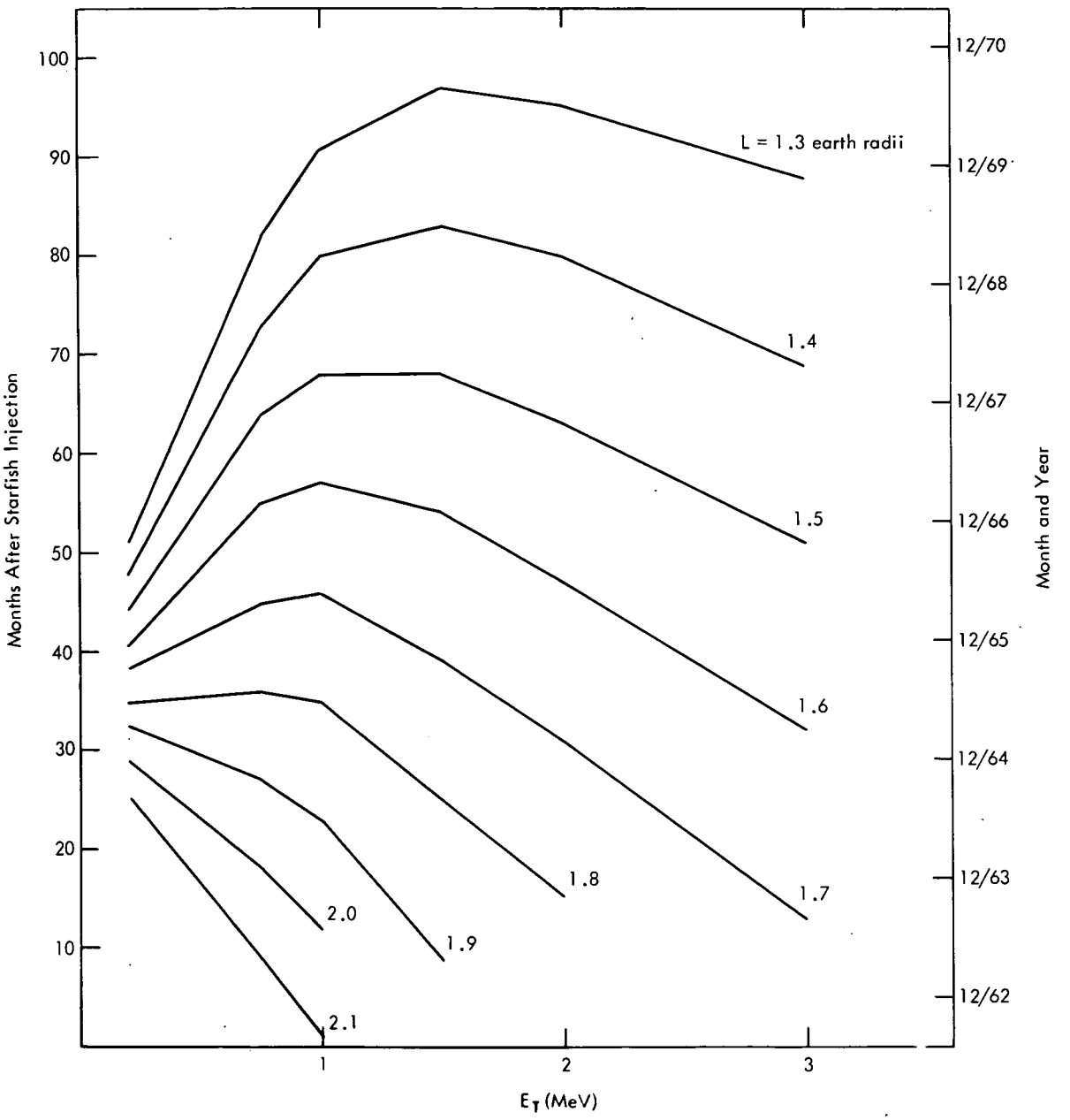

Figure 14. Cutoff Times - Method 2

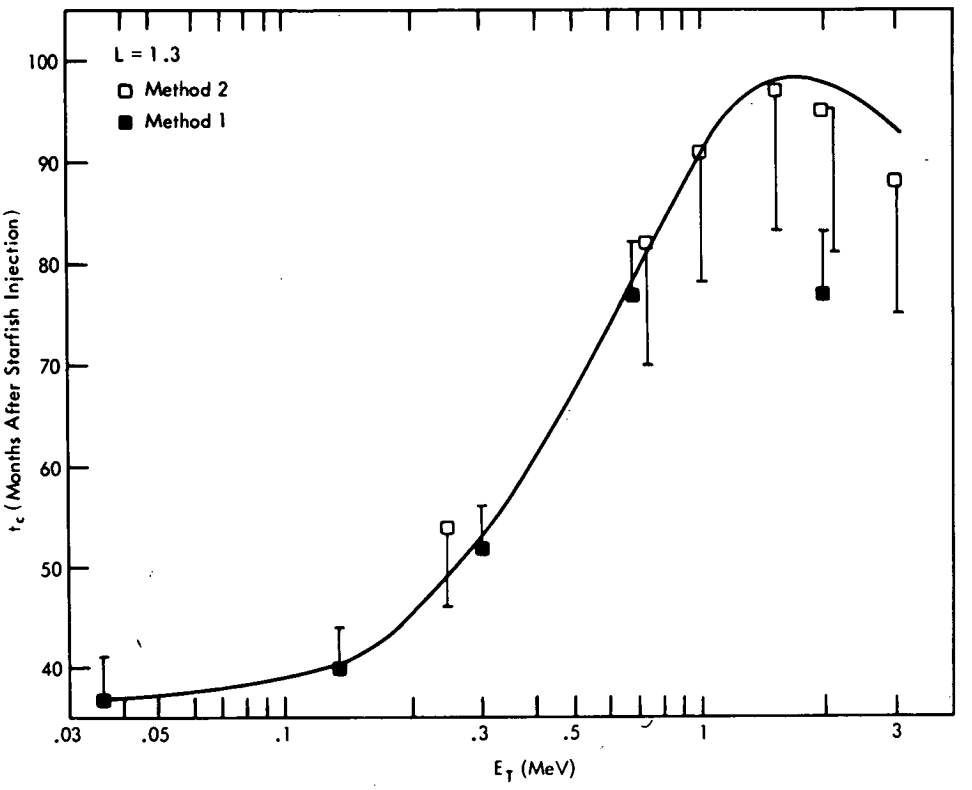

Figure 15. The Cutoff Time Model

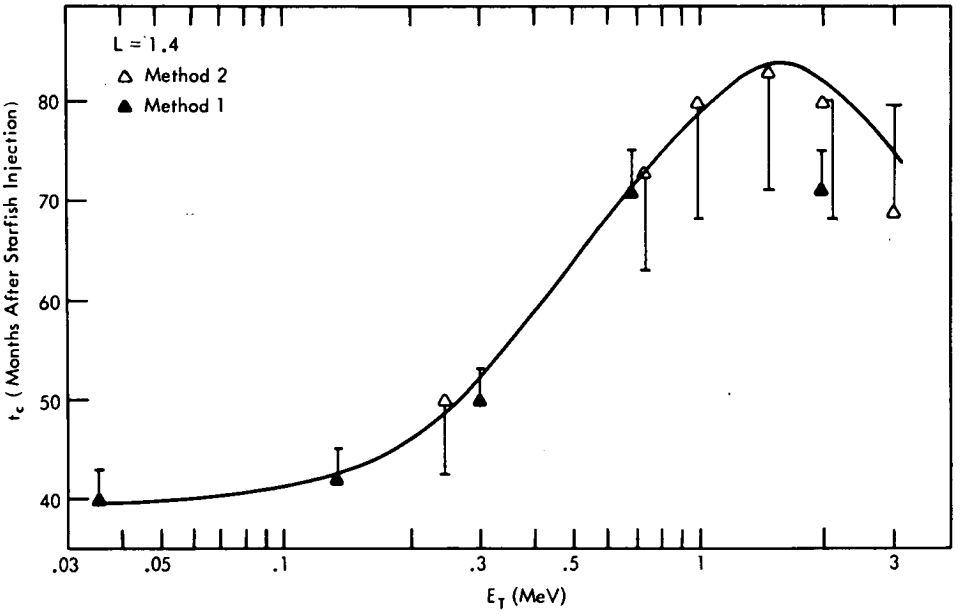

Figure 16. The Cutoff Time Model

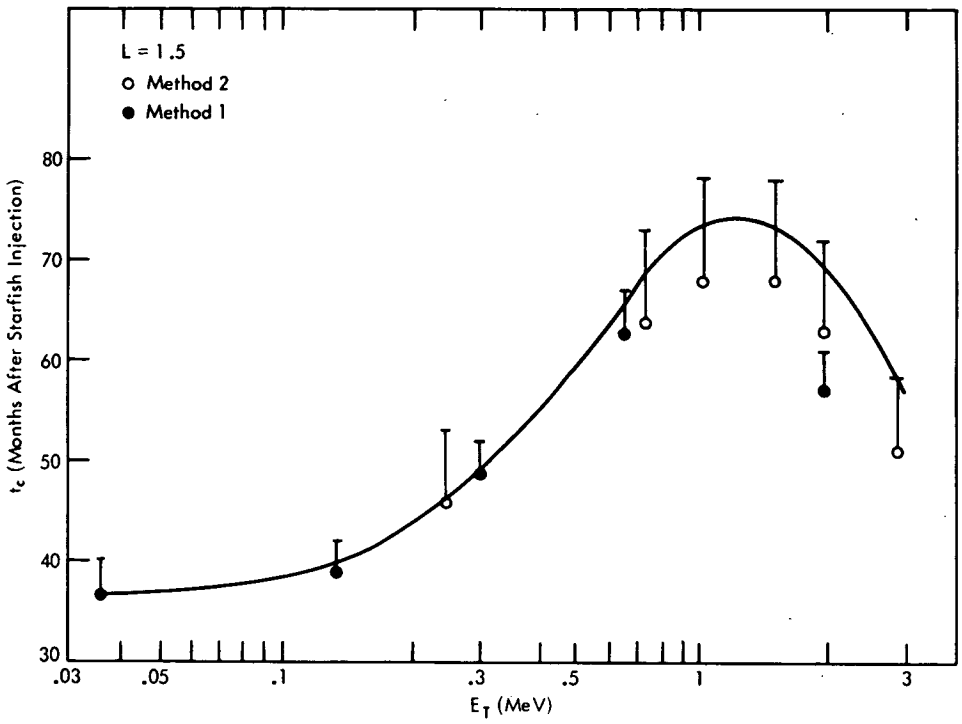

Figure 17. The Cutoff Time Model

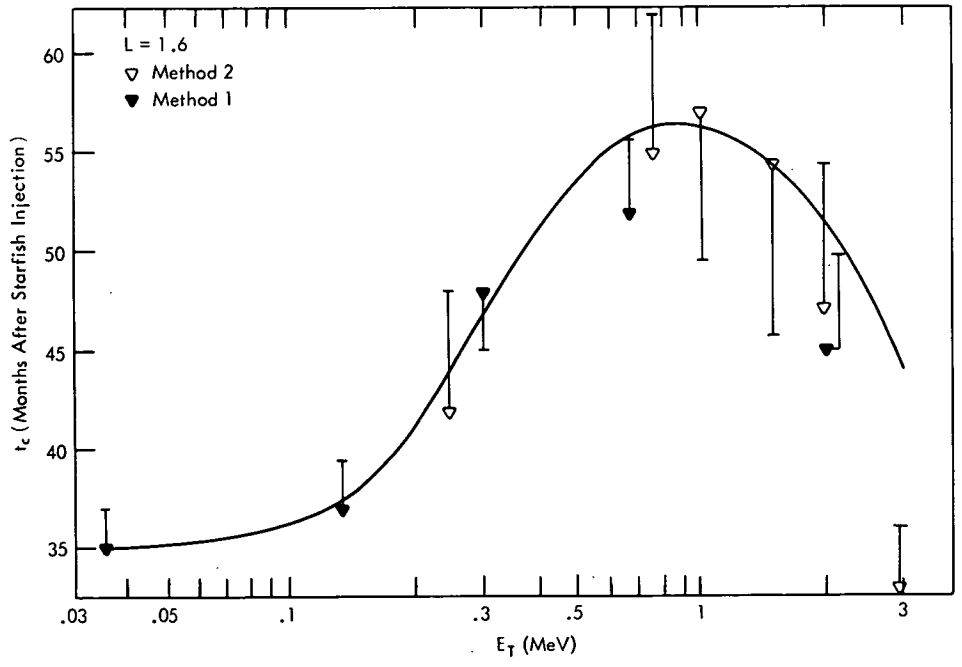

Figure 18. The Cutoff Time Model

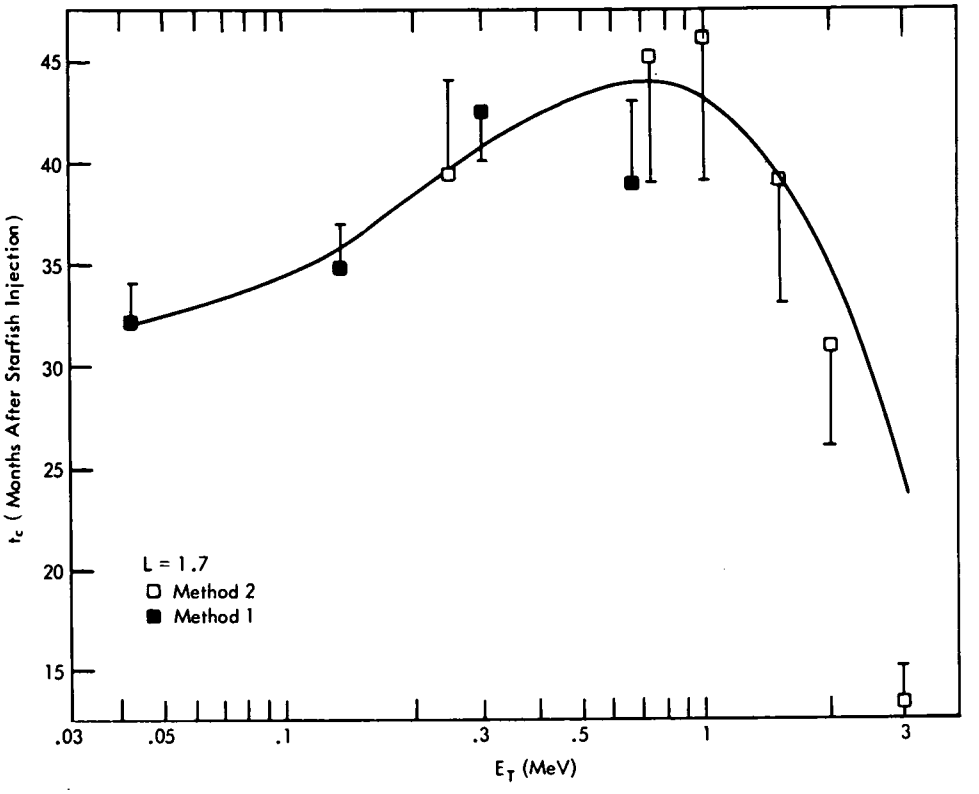

Figure 19. The Cutoff Time Model

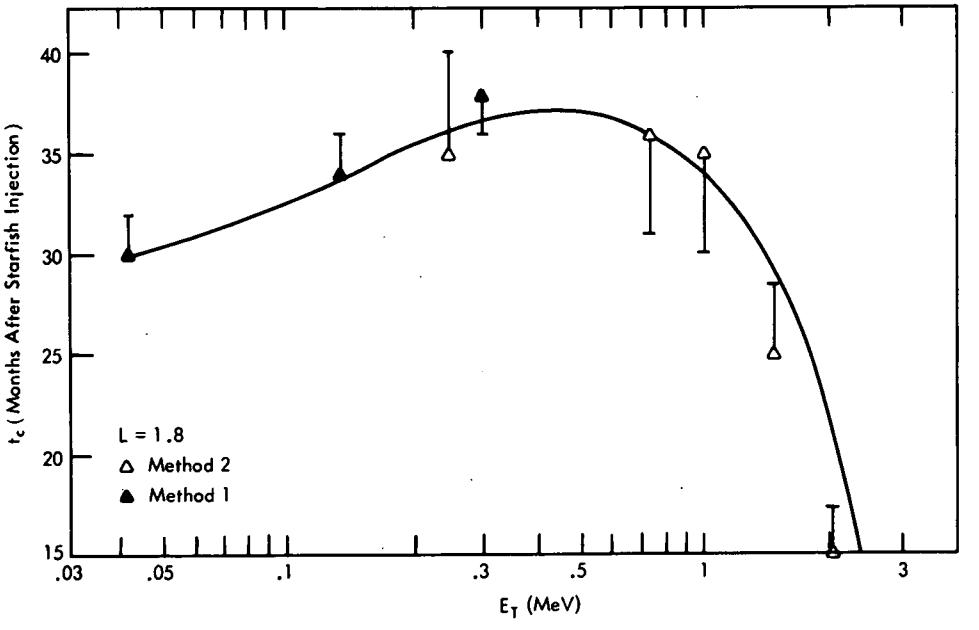

Figure 20. The Cutoff Time Model

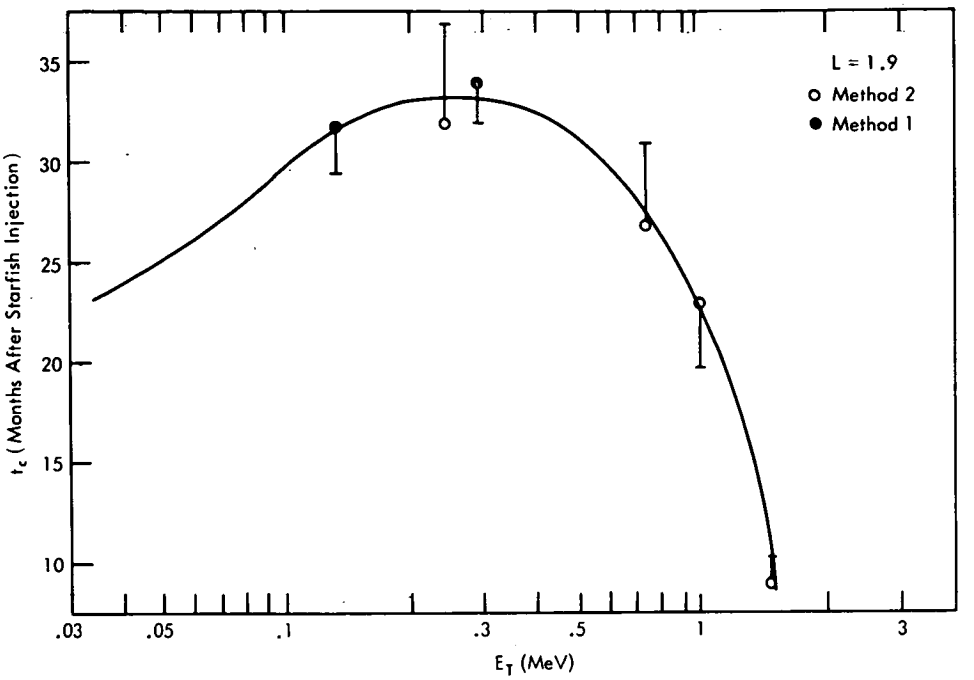

Figure 21. The Cutoff Time Model

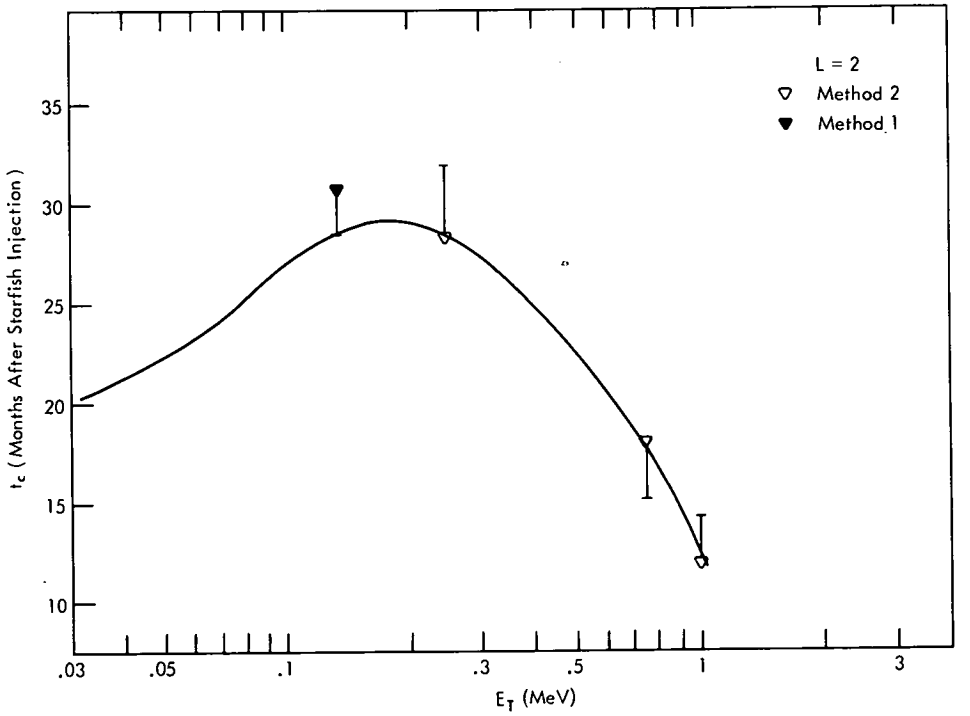

Figure 22. The Cutoff Time Model

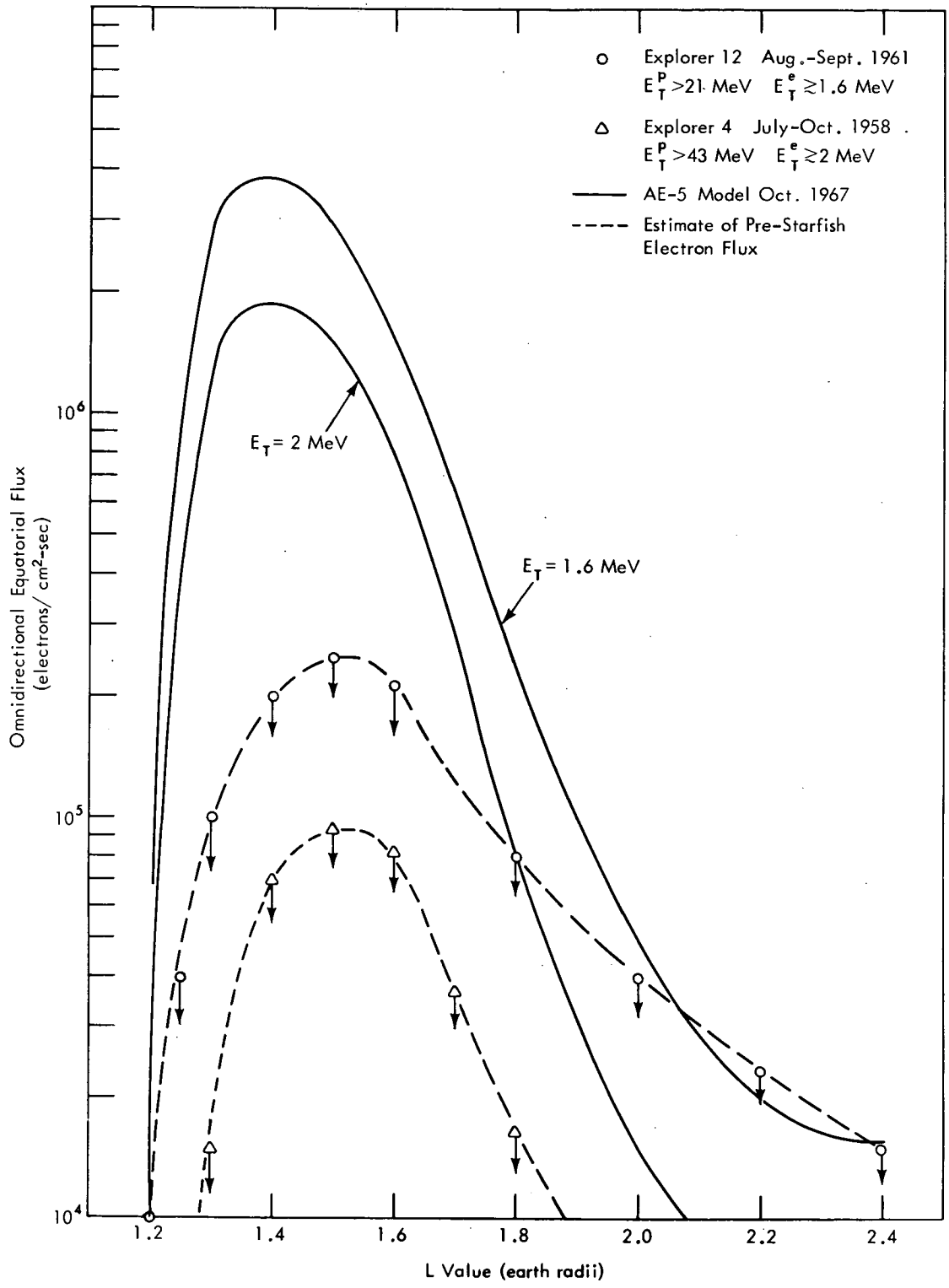

Figure 23. Pre-Starfish Electron Flux Estimates

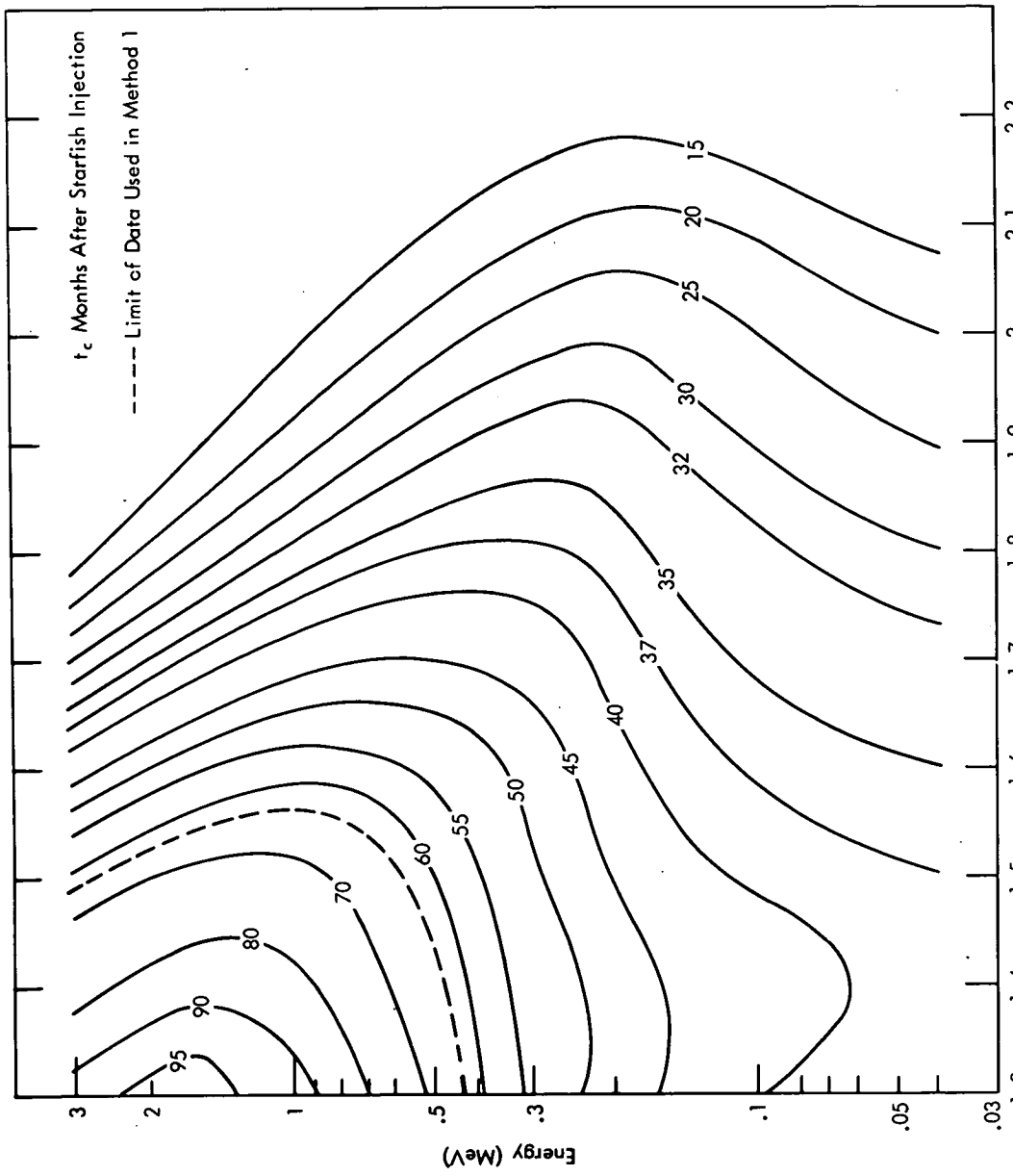

Figure 24. Constant Cutoff Time Contours

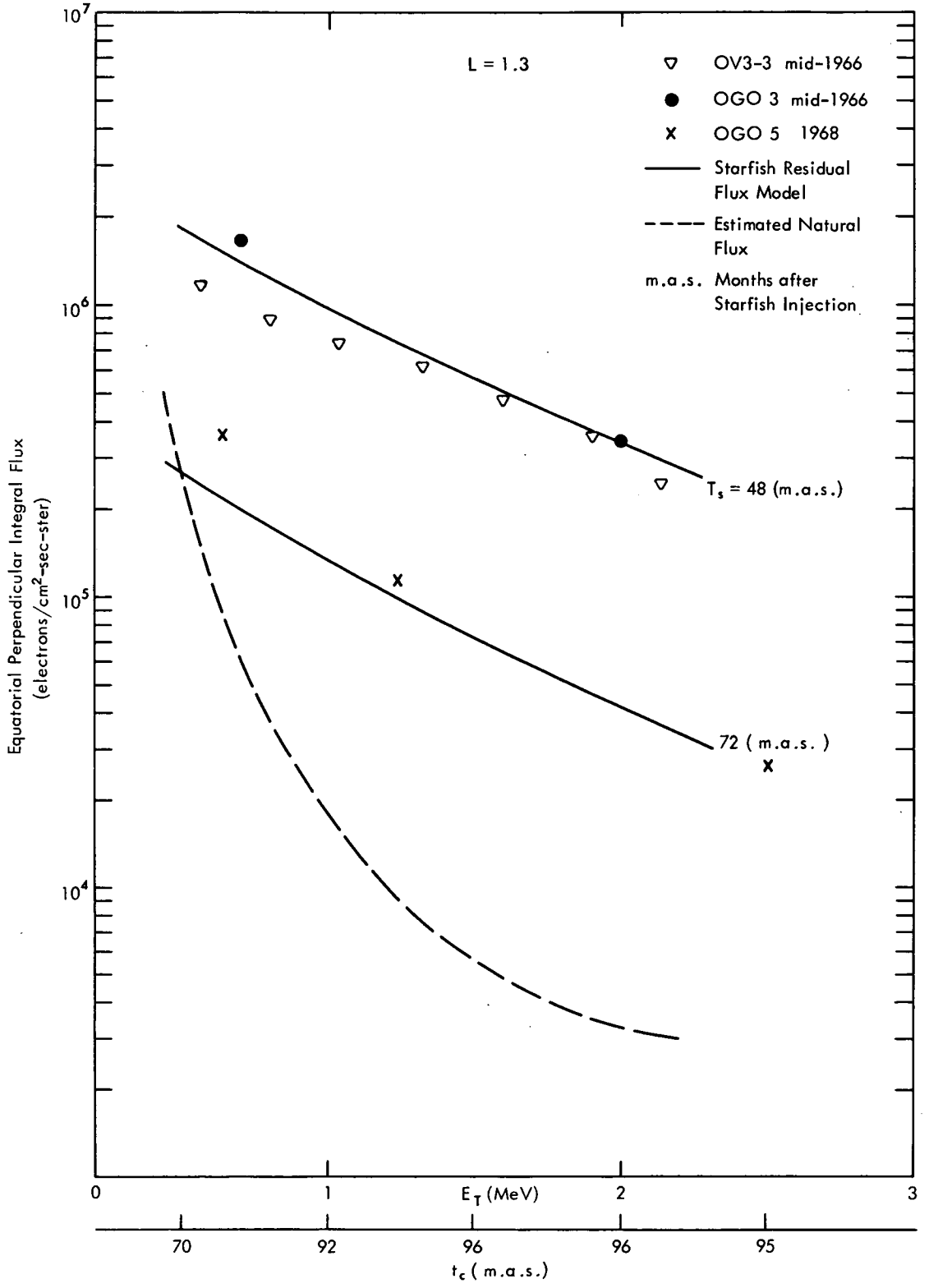

Figure 25. The Starfish Decay Process at High Energies

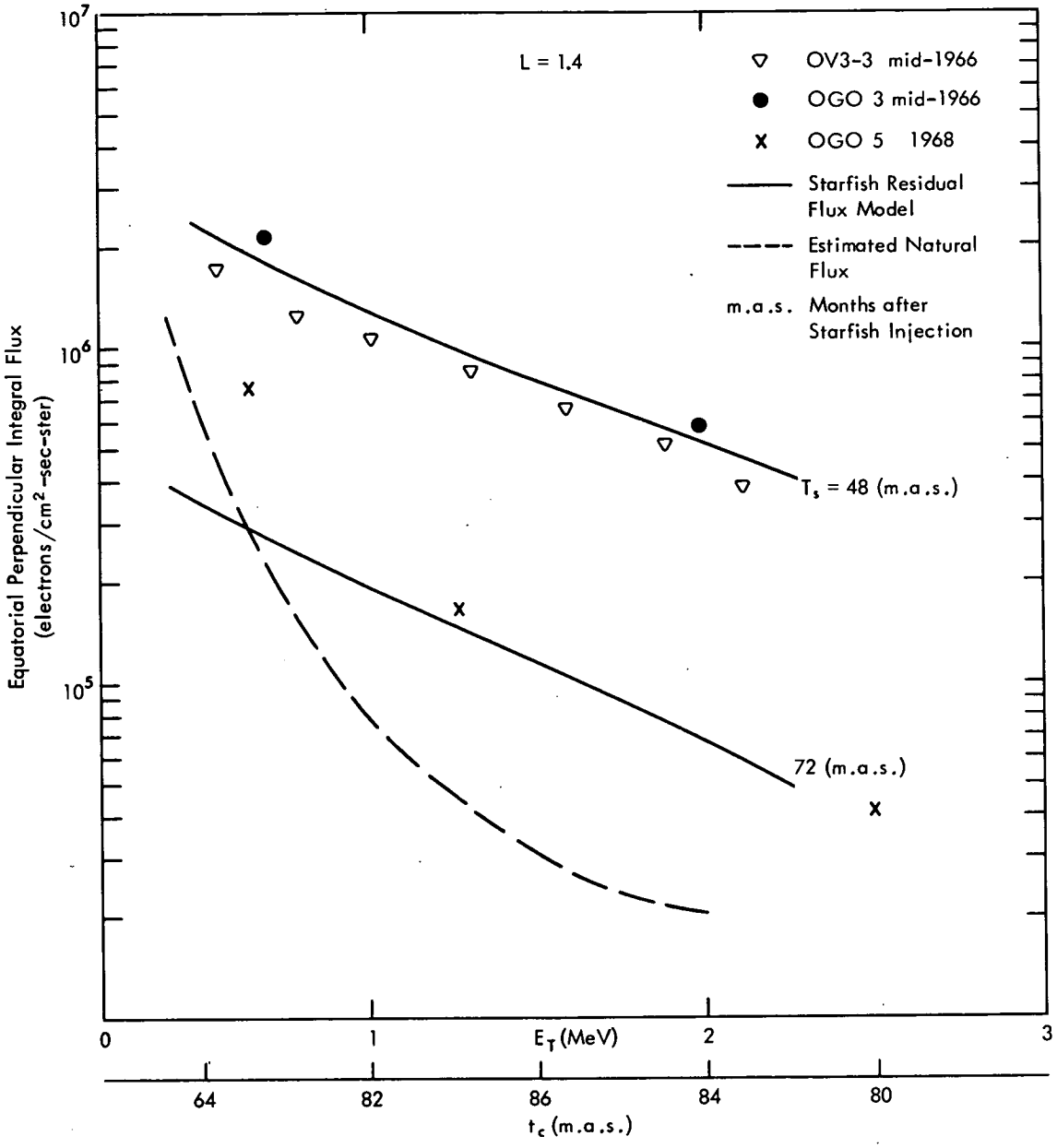

Figure 26. The Starfish Decay Process at High Energies

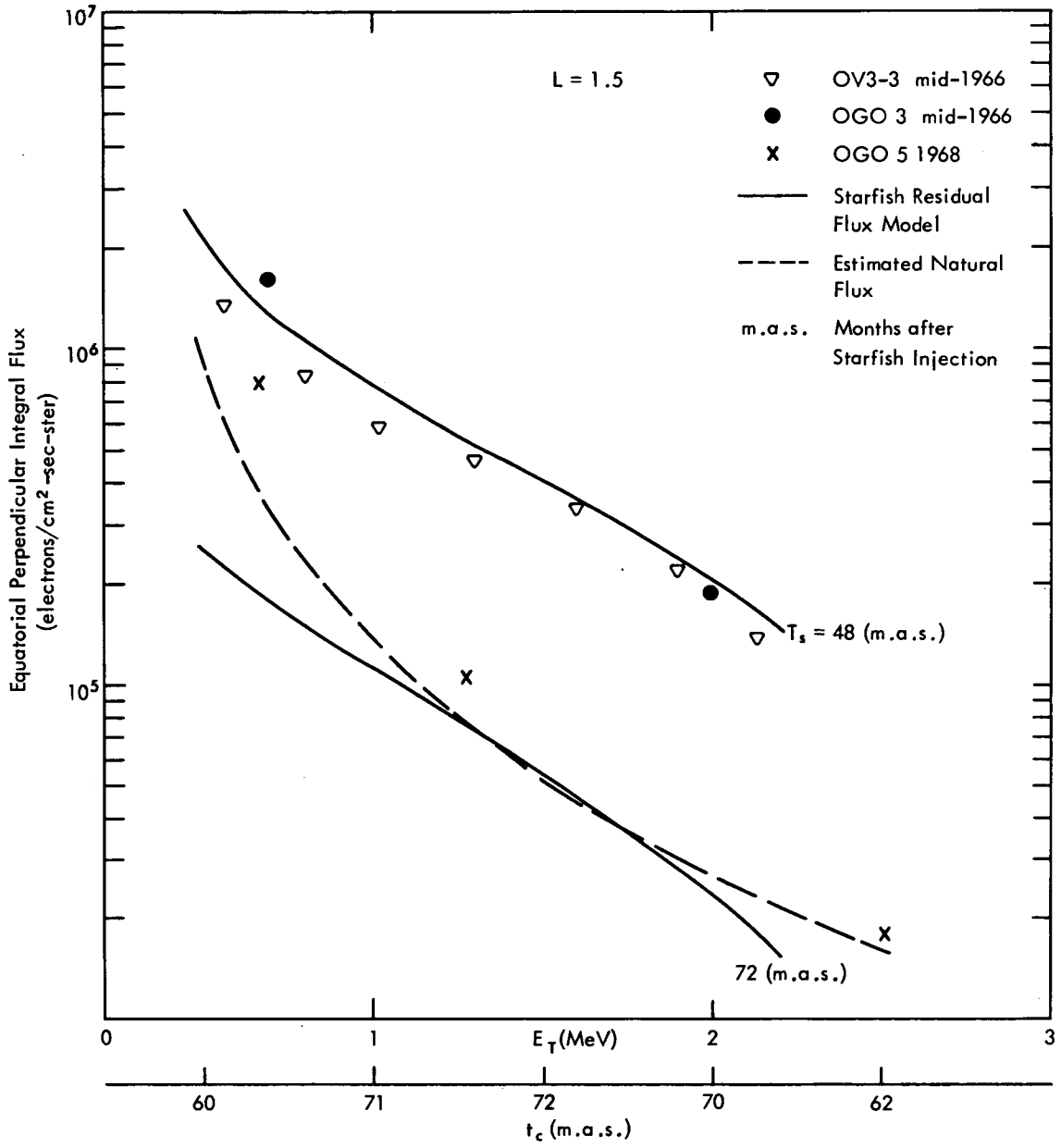

Figure 27. The Starfish Decay Process at High Energies

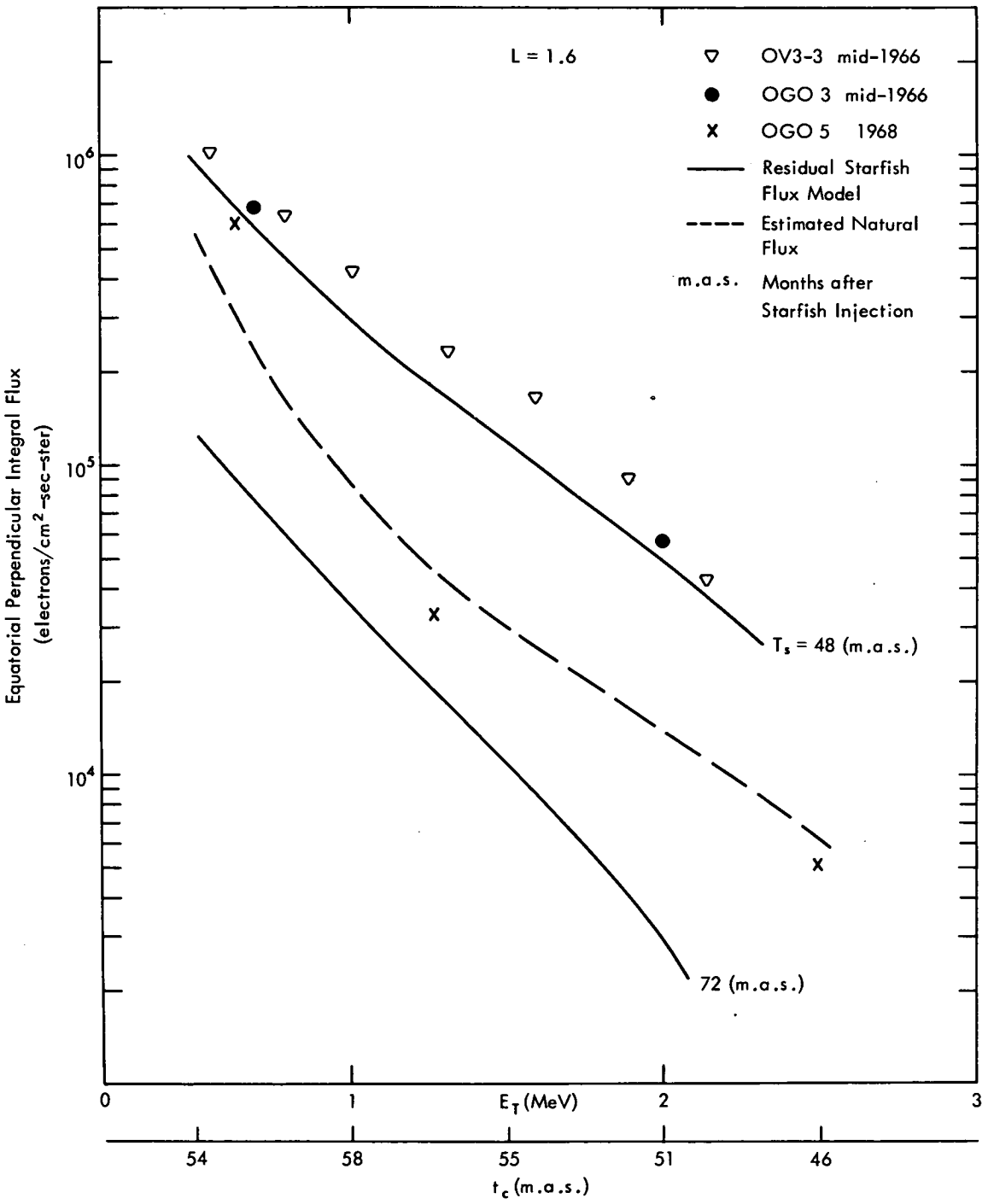

Figure 28. The Starfish Decay Process at High Energies

* U.S. GOVERNMENT PRINTING OFFICE: 1972-735-967/603